

RIPPLE++: An Incremental Framework for Efficient GNN Inference on Evolving Graphs ^{*}

Pranjal Naman¹, Parv Agarwal¹, Hrishikesh Haritas¹ and Yogesh Simmhan¹²

*Department of Computational and Data Sciences (CDS),
Indian Institute of Science (IISc),
Bangalore 560012 India*

Email: {pranjalnaman, simmhan}@iisc.ac.in

Abstract

Real-world graphs are dynamic, with frequent updates to their structure and features due to evolving vertex and edge properties. These continual changes pose significant challenges for efficient inference in graph neural networks (GNNs). Existing *vertex-wise* and *layer-wise* inference approaches are ill-suited for dynamic graphs, as they incur redundant computations, large neighborhood traversals, and high communication costs, especially in distributed settings. Additionally, while sampling-based approaches can be adopted to approximate final layer embeddings, these are often not preferred in critical applications due to their non-determinism. These limitations hinder low-latency inference required in real-time applications. To address this, we propose RIPPLE++, a framework for streaming GNN inference that efficiently and accurately updates embeddings in response to changes in the graph structure or features. RIPPLE++ introduces a generalized incremental programming model that captures the semantics of GNN aggregation functions and incrementally propagates updates to affected neighborhoods. RIPPLE++ accommodates all common graph updates, including vertex/edge addition/deletions and vertex feature updates. RIPPLE++ supports both single-machine and distributed deployments. On a single machine, it achieves up to 56K updates/sec on sparse graphs like Arxiv (169K vertices, 1.2M edges), and about 7.6K updates/sec on denser graphs like Products (2.5M vertices, 123.7M edges), with latencies of 0.06–960ms, and outperforming state-of-the-art baselines by 2.2–24 \times on throughput. In distributed settings, RIPPLE++ offers up to $\approx 25\times$ higher throughput and 20 \times lower communication costs compared to recomputing baselines.

1 Introduction

Graph Neural Networks (GNNs) [23] have the ability to learn low-dimensional representations that capture both the topology and attributes of graph datasets. Unlike traditional neural networks that assume grid-like inputs (e.g., images or sequences), GNNs can capture both the vertex/edge features and the topological structure by aggregating and transforming a vertex’s multi-hop neighbors into embeddings for training. This ability to learn expressive features in the property graph, and use them for inference tasks such as vertex labeling, subgraph labeling, link prediction, etc., makes GNNs a powerful tool. It is used in wide-ranging linked data applications: for detecting financial frauds [14,25], predicting traffic flow [16], analyzing social networks [23,46], and making e-commerce recommendations [8,9,27,43].

^{*} Extended full-length version of paper that appeared at ICDCS 2025: “*RIPPLE: Scalable Incremental GNN Inferencing on Large Streaming Graphs*”, Pranjal Naman and Yogesh Simmhan, in International Conference on Distributed Computing Systems (ICDCS), 2025. DOI: <https://doi.org/10.1109/icdcs63083.2025.00088>

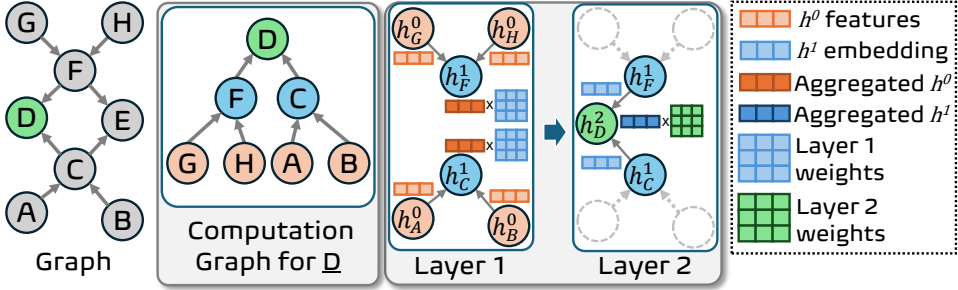


Figure 1: GNN inference on static graphs for vertex D . h_D^2 is the final layer embedding that maps to a predicted label.

Such applications frequently operate on *large-scale graphs*, consisting of millions to billions of vertices and edges, e.g., financial platforms monitor millions of real-time transactions between users, and urban traffic systems manage sensor data from hundreds of thousands of junctions. These settings often impose real-time latency requirements during GNN inference [1, 24, 42, 50]. For instance, a delay in identifying suspicious transactions in financial networks can allow fraudulent activities to occur, leading to financial loss. Similarly, delays in real-time traffic flow prediction used for traffic signal optimization can exacerbate congestion during peak hours.

1.1 GNN Inference on Static Graphs

GNN inference involves performing a forward pass through the trained Neural Network (NN) model. When, say, predicting the label for vertex D in Fig. 1, we compute its L -hop in-neighbors (called the *computational graph*), and then propagate the aggregated leaf features to the input layer of the L -layer NN to generate embeddings for the penultimate level of the computation graph. We pass these embeddings higher up the tree as we pass through each NN layer. The final prediction for the vertex is the final-layer embedding produced by this forward pass.

When inference has to be done with low latency, the simplest approach is to perform a forward pass once on all graph entities using the trained GNN model, cache the predicted results, and return them rapidly using a simple lookup [47].

There are two approaches for generating the final layer embeddings in a static graph. *Vertex-wise* inference (Fig. 2, center) is akin to just performing the forward pass of GNN training (training also includes the backward pass to update weights). The embeddings within an L -hop neighborhood of each target vertex (*green*) being labeled are aggregated, assuming a vertex labeling GNN task. During training, the neighborhood of the computational graph is randomly sampled to keep the subgraph size manageable and still achieve good model accuracy [17]. However, such sampling affects the correctness and *deterministic* nature of the predictions if done during inference [20], making it unsuitable for many real-world applications due to both *non-determinism and approximation*, e.g., the same transaction should be classified as a fraud across multiple inference requests, in the absence of other changes. Fig. 3 shows this trade-off for the Reddit social network graph (233K vertices, 114M edges; experiment setup described in § 6.1). As the sampling fanout size increases, we get a better and more predictable accuracy (*left y-axis*, box plots) but also a higher per-vertex average inference time (*right y-axis*, red marker). Guaranteeing both deterministic and accurate predictions requires the entire L -hop neighborhood to be considered during inference, which can lead to *neighborhood explosion* [17], with significantly higher memory and computational demands.

So, a *layer-wise* inference approach (Fig. 2, right) is typically employed for bulk processing [47]. Here, the embeddings for each hop (colored vertex layers) are computed for all vertices in the graph and used as inputs to calculate the embeddings for the next layer (*orange to blue to green*). This avoids the explosion in computational graph sizes by leveraging overlaps in vertices

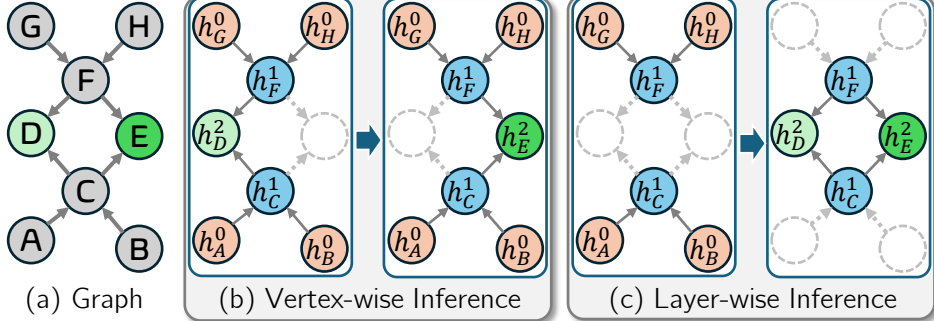


Figure 2: *Vertex-wise* vs. *Layer-wise* inference on static graphs.

at the same layer with the neighborhoods of proximate vertices, and prevents redundant computation, which occurs in vertex-wise inference, e.g., h_F^1 and h_C^1 are recomputed for inference of D and E but computed only once in layer-wise.

1.2 GNN Inference on Evolving Graphs

GNN inference becomes even more complex when operating on graphs that *evolve continuously* in the presence of vertex/edge additions/deletions, or changes to their features [4,37]. E.g., a friend being added or removed in a social network causes an edge addition/deletion [3]; changing traffic flows in a road network updates an edge feature [16], transactions in a fintech network change the account-balance vertex feature [36]. Thousands of such dynamic graph mutations can occur per second, affecting the output of GNN predictions for entities in their neighborhood [2,30,44]. However, performing *layer-wise* inference on the *whole graph* every time an update (or a small batch of updates) occurs is too time-consuming for latency-sensitive applications. Instead, we can limit the recomputation of the vertex labels only to those that fall within the L -hop out-neighborhood (*affected neighborhood*) of entities that have been updated in the graph.

Notably, the extent of these cascading effects grows with the average degree of the graph and the number of updates applied in a batch, as more entities fall within the affected neighborhood of the modified vertices. E.g., in Fig. 4, the fraction of vertices affected for the *Arxiv* graph (average vertex degree of 6.9) increases from 0.06% to 2.2% of the total vertices, as the batch size (bs) increases from 1 to 100. However, for the *Products* graph (degree 50.5), the growth is sharper, from 0.7% to $\approx 37\%$. This also directly impacts the *latency* to translate incoming graph updates into updated GNN embeddings and inversely affects the *update throughput* that can be supported. As the affected neighborhood size increases, so does the per-batch latency to perform *inference recomputations (RC)* upon updates, growing from 5.5ms to ≈ 110 ms for *Arxiv* using bs from 1–100, and from ≈ 260 ms to 11.3s for *Products*. The throughput of updates processed to give fresh GNN predictions is 177–916 up/s for *Arxiv* but only 3.7–8.8 up/s for *Products*.

1.3 Large Memory Requirements of Layer-wise Inference

Layer-wise GNN inference requires the whole graph and its embeddings to be present in memory¹. But graphs such as *Papers* (111M vertices, 1.6B edges, 128 features) [18] and their embeddings can easily take > 128 GiB of RAM. Another significant challenge in handling real-world workloads is the immense scale of the graph data. As the graph sizes grow, managing the inference process on a single machine becomes more challenging due to the increased memory demands.

¹Interestingly, layer-wise GNN inference does not benefit much from using GPUs since the computational load is modest (Fig. 19 in Appendix). Instead, computation on CPUs offers comparable performance and also benefits from the available larger host memory.

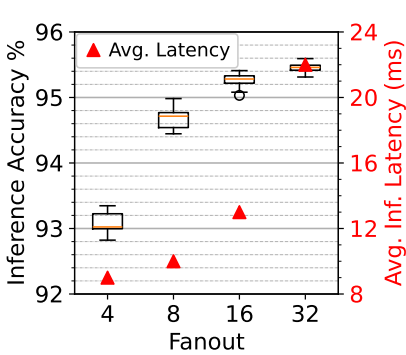


Figure 3: Effect of neighborhood sampling on vertex-wise inference accuracy and latency (Reddit graph, 3-layer SAGEConv).

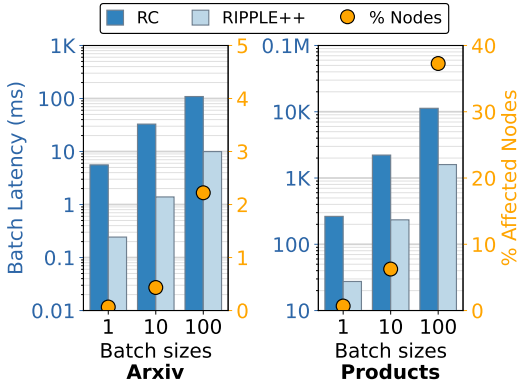


Figure 4: % of affected vertices and inference latency per batch-update, for Ripple++ (RP) and baseline RC, with differing batch sizes (3-layer GraphConv).

This necessitates efficient *distributed execution* of incremental computation on a compute cluster to support larger graphs.

Recent works like InkStream [42], that also perform incremental GNN inference like us, only support graph edge updates, work with fewer GNN architectures, and lack a distributed execution model for scaling to larger graphs.

1.4 Contributions

In this paper, we present Ripple++, a low-latency framework for streaming GNN inference that efficiently handles real-time updates to large-scale graphs using incremental computation. It uniquely applies a delta to undo previous embedding aggregations, and redo them using updated embeddings to sharply reduce any recomputation. Ripple++ offers both a single-machine and a distributed execution model. Our technique *avoids redundant computation* of embeddings for the entire neighborhood of updates and instead, scopes it to just a subset of the operations. In particular, when one (or a few) vertices (V') among the in-neighbors (V) of another vertex (u) get updates, rather than aggregate the embeddings from all V vertices, we *incrementally aggregate* only the deltas from the updated vertices V' . This reduces the number of computations from $k = |V|$ to $k' = |V'|$, which is often an order of magnitude smaller. Further, we support diverse mutations such as vertex/edge/feature updates and GNNs with linear, non-linear, and attention-based aggregation, while guaranteeing deterministic and accurate behavior, along with a distributed execution model for large graphs, unlike SOTA approaches [42] that only support edge-level updates and on only a single machine.

Specifically, we make the following contributions:

1. We propose Ripple++, a scalable incremental GNN inference framework that supports streaming edge and vertex additions and deletions, and feature updates, for GNN models that can include *monotonic* and *accumulative* aggregators, and also *attention-based* architectures (§ 3).
2. We present a detailed analytical comparison of our incremental approach (Ripple++) against full recomputation (RC), characterizing the conditions under which incremental inferencing offers best benefits (§ 3.5).
3. We design a locality-aware routing strategy to place new vertices, which minimizes edge cuts and improves distributed execution under graph evolution compared to hash-based routing (§ 4.4).

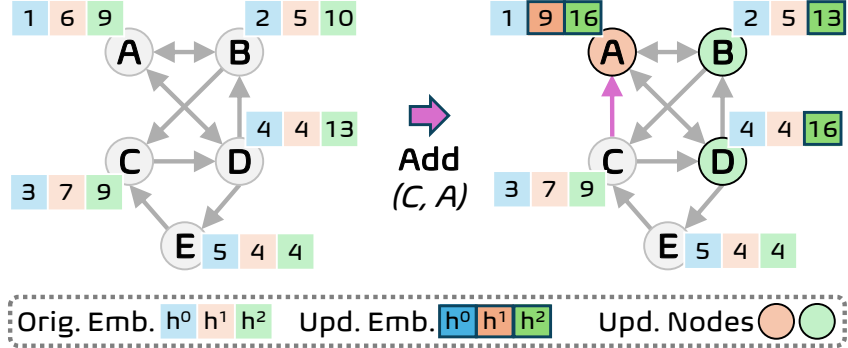


Figure 5: Cascading effect on the vertex embeddings due to an edge addition during 2-layer GNN inference.

4. We perform detailed experiments of RIPPLE++ on four real-world graphs with 169K–111M vertices and 1.2M–1.6B edges, for seven workloads across four GNN models and aggregation functions. We also compare it against other recomputation strategies and a state-of-the-art (SOTA) framework, InkStream [42]. RIPPLE++ achieves up to 56K up/s inference throughput on a single-machine that is 2.2–24× faster than InkStream, and 25× improvement over the recompute baseline in a distributed setting (§ 6).

We also provide background on GNN training and inference (§ 2), contrast RIPPLE++ with related works (§ 7), and conclude with a discussion of future directions (§ 8).

In a prior conference paper [34], we introduced the key ideas of incremental GNN inference in RIPPLE. This article significantly extends it as RIPPLE++: (1) We generalize the incremental technique to support complex GNN architectures with monotonic operators (e.g., max) and graph-attention (e.g., GAT), beyond just *accumulative* operators supported earlier; (2) We extend the design to support vertex additions and deletions, to complement edge/vertex feature updates supported earlier; (3) We offer a detailed analysis of incremental inferencing against full-recompute, identifying the scenarios where we offer the most benefit; (4) We propose a locality-aware update routing to reduce edge-cuts and improve load balancing in a distributed setting, which goes beyond our earlier hash-based routing; and (5) We substantially expand the experiments with two new hybrid incremental GNNs, study the effect of number of GNN layers, scale the evaluation to 20M updates, and compare against the SOTA InkStream work [42]. These make RIPPLE++ a general and scalable platform for low-latency GNN inference on large evolving graphs.

2 Background

2.1 Training vs. Inference of Graph Neural Networks

GNNs are trained using iterative forward and backward passes, similar to Deep Neural Networks (DNNs). During the *forward pass*, when training over a labeled vertex u , the layer- l of an L -layer GNN uses the AGGREGATE function to accumulate the $(l-1)$ embeddings of the neighbors $\mathcal{N}(u)$ of the vertex (Fig. 1). The aggregated embedding vector x_u^l is then processed by an UPDATE function, which is the learnable component of the network, and passed through a nonlinear function σ . This repeats L -times, once per layer, to get the final layer embedding h^L for the training vertex. This ends the forward pass. We then do a *backward pass* across L layers to update the learnable parameters using a loss function.

$$x_u^l = \text{AGGREGATE}^l(\{h_v^{l-1}, v \in \mathcal{N}(u)\}) \quad (1)$$

$$h_u^l = \sigma(\text{UPDATE}^l(h_u^{l-1}, x_u^l)) \quad (2)$$

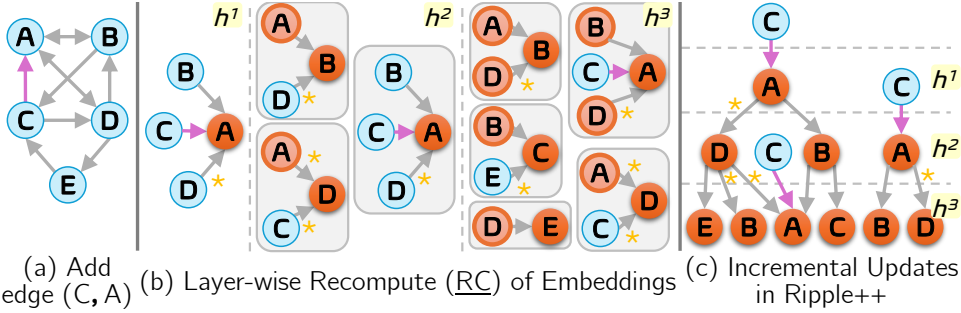


Figure 6: Recomputation and Ripple++’s Incremental Comp. on Edge addition. Dark orange vertices update their embeddings in a hop (3-layer GNN). Edges with ‘ $*$ ’ indicate remote messages passed between machines during distributed execution across partitions $\{A, B, C\}$ and $\{D, E\}$, discussed in § 4.

During GNN inference, only the forward pass is performed to compute the final layer embedding for the target vertex, which maps to the predicted label. For static graphs, this can be pre-calculated, thus avoiding compute at inference time.

2.2 Inference on Streaming Graphs

Unlike for static graphs, pre-calculating the final layer embeddings and labels for all vertices is not beneficial for dynamic graphs. Each update to a vertex or edge triggers a cascade of embedding updates across multiple vertices at each hop, ultimately changing the embeddings and, consequently, the predicted labels of all vertices at the final hop.

Fig. 5 shows a unit-weighted graph with pre-calculated embeddings for a 2-layer GNN with *sum* as the aggregator. When edge (C, A) is added, the h_A^1 and h_A^2 embeddings of A get updated, which cause cascading updates to the h^2 embeddings of $\{B, D\}$, possibly changing the predicted labels of $\{A, B, D\}$ in the final hop. Notably, the embeddings of C and E remain unaffected. Any change in the graph topology or the vertex features only *ripples* through to a maximum of L -hops, for an L -layer GNN. So, it is not necessary to update the embeddings of *all* vertices. The fraction of affected vertices per batch can span from $< 3\%$ of vertices for *Arxiv* to $\approx 37\%$ of vertices for *Products* (Fig. 4). At the same time, it is crucial to propagate the effect of the dynamic graph updates quickly and accurately for timely inference.

We can classify the inference of streaming graphs into trigger-based and request-based. *Trigger-based* inference immediately notifies the application of any changes to the predicted vertex label due to graph updates. In contrast, *request-based* inference follows a pull-based model, where the application queries the label of a specific entity in the graph as needed. Both classes have unique requirements and different strategies, e.g., update propagation can be done lazily for rarely accessed vertices in the graph for the request-based inference model. In this paper, we tackle trigger-based inference.

2.3 Aggregation Functions

In a multi-layered GNN, the *neighborhood aggregation* forms a key operation, where each vertex combines the information from its neighbors to generate its representation using Eqn. 1. Existing research on GNNs often uses *linear accumulative* functions like *sum*, *mean*, or *weighted sum* based on edge weights or edge attention; occasionally, they consider *non-linear monotonic* aggregation functions like *max* or *min*. Kipf et al. [23] propose the Graph Convolution Network (GCN) architecture, which adopts a weighted summation aggregation, while GraphSAGE [17] typically uses sum or mean. Graph Attention Networks (GAT) [38] follow an attention-based summation where the attention on an edge is calculated based on the features of the participating vertices. Xu et al. [45] show that the expressiveness of the sum aggregator overshadows

Table 1: Popular Aggregation functions in GNNs.

Aggregation Fn.	Definition	Used By
<i>sum</i>	$\mathbf{h}_i = \sum_{j \in \mathcal{N}(i)} \mathbf{h}_j$	[17] [45] [12]
<i>mean</i>	$\mathbf{h}_i = \frac{1}{ \mathcal{N}(i) } \sum_{j \in \mathcal{N}(i)} \mathbf{h}_j$	[17] [12]
<i>max/min</i>	$\mathbf{h}_i = \max_{j \in \mathcal{N}(i)} \mathbf{h}_j$	[17] [12]
<i>weighted sum</i>	$\mathbf{h}_i = \sum_{j \in \mathcal{N}(i)} \alpha_{ij} \cdot \mathbf{h}_j$	[23]
<i>attention</i>	$\mathbf{h}_i = \sum_{j \in \mathcal{N}(i)} \alpha(\mathbf{h}_i, \mathbf{h}_j) \cdot \mathbf{h}_j$	[38]

other functions, and use this in Graph Isomorphism Networks (GIN). Dehmamy et al. [12] and Corso et al. [11] show that the expressive power of a GNN module can be increased by using a combination of aggregators, e.g., the former uses a combination of sum and mean, while the latter uses both linear and non-linear aggregators. With this in mind, we support a variety of such aggregation functions across multiple GNN architectures (Table 1).

3 RIPPLE++ System Design

In this section, we present the design for RIPPLE++, a GNN inference framework for streaming graphs that supports *trigger-based* applications that need to be notified of changes to the predictions of any graph entity upon receiving updates as soon as possible. RIPPLE++ uses incremental computation over a batch of updates, intelligently using the delta in prior embeddings to avoid redundant computation of parts of the computation neighborhood. RIPPLE++ supports both an efficient single-machine execution if the entire graph, its features and embeddings fit in the RAM of a single server, and a distributed execution to scale to larger graphs with efficient communication primitives.

3.1 Preliminaries

We make certain simplifying assumptions when designing RIPPLE++. The GNN model used for inference has L layers. As bootstrap, the initial embeddings have been calculated for all existing graph entities prior to new updates streaming in. Each vertex $u \in V$ has its features h_u^0 and intermediate and final layer embeddings h_u^l ($l \in [1, L]$). The initial embedding matrices, $H_{T_0}^l$ of layer l , are generated using the GNN model and stored, and the current labels of all vertices can be extracted from $H_{T_0}^L$. These serve as starting points when new updates arrive.

RIPPLE++ is designed for GNN model architectures that support either *linear accumulative*, *non-linear monotonic*, or attention-based aggregation functions (Table 1). RIPPLE++ works in one of two incremental modes – *completely incremental* or *hybrid incremental*, which we describe later. We use a GNN model for vertex classification as the running example, though this can be extended to other vertex- or edge-based tasks. RIPPLE++ supports five types of updates: *edge additions*, *edge deletions*, *vertex additions*, *vertex deletions*, and *vertex feature changes*.

We assume that updates arrive *continuously* and are *batched* into fixed batch sizes (bs) that are then applied to the graph, triggering (incremental) computation of the affected entities. The updated predictions are immediately made available to the consumers. Since we assume a high update rate of 100–1000 updates per second (up/s), this bulk operation amortizes the overheads, reduces redundant computation, and achieves higher throughput. The size of the batch is a hyperparameter that can be tuned to trade-off update throughput against batch execution latency. We evaluate RIPPLE++ for different batch sizes in our experiments, which in the future can guide the selection of dynamic batch sizes.

3.2 Layer-wise Update Propagation through Recomputation

We first describe a competitive baseline approach that performs *layer-wise recomputing (RC)*, scoped to the neighborhood of updates. When an edge/vertex/feature is updated, it causes cascading updates, starting from the *root vertex* on which the update is incident and on the embeddings within the L -hop neighborhood (Fig. 5).

An *edge addition* (u, v) immediately alters the h_v^1 embedding of the sink vertex v , which leads to further downstream changes. E.g., in Fig. 6(b), adding the edge $C \rightarrow A$ initially changes only the h_A^1 embeddings of sink vertex A at hop distance 1 from the root vertex C . But recomputing h_A^1 requires fetching the h_0 embeddings of *all* the in-neighbors of A : h_B^0 , h_C^0 and h_D^0 , and aggregating them, followed by the update operation.

Similarly, for the next layer of updates to h^2 embeddings, the update to h_A^1 cascades to all out-neighbors $\{B, D\}$ for A , causing h_B^2 and h_D^2 to be updated by aggregating the new value of h_A^1 and prior value of h_D^1 for the neighbor B , and the new value of h_A^1 and prior value of h_C^1 for neighbor D . In addition, the addition of the $C \rightarrow A$ edge will also cause the h_A^2 embeddings for A to get updated, aggregating the new edge embedding from h_C^1 and prior values of h_B^1 and h_D^1 . Hence, recomputation of the h^2 embeddings requires pulling the h^1 embeddings of all the in-neighbors of the affected vertices, A, B , and D . Similarly, the h^3 embeddings of the out-neighbors of $\{A, B, C, D, E\}$ will be updated by pulling the h^2 embeddings of their neighbors and recomputing the aggregation function over all of them, followed by the update function. These cascading changes are illustrated by the orange vertices in Fig. 6(b) at each layer.

An *edge deletion* will traverse from the source vertex as the *root*, and affect the same set of vertices at each hop as above. It requires similar recomputations, except now there will be *one less neighbor* when updating h_v^l . The embedding update to h_v^1 will cause a similar cascading set of changes to downstream vertices. E.g., if edge $C \rightarrow A$ is removed at a later time, the only vertex whose h^1 embedding changes is A , followed by a similar propagation as when the edge was added.

A *vertex addition* in itself should not trigger any updates, except to update its own embeddings. However, vertices can be created as a part of an edge addition. So, adding a vertex u can trigger the same traversal from root u as when an edge (u, v) is added, if the sink vertex v already exists but the source vertex u needs to be created. But, if u is the sink vertex of an added edge, only its own embedding is affected, as no downstream vertices exist to traverse to.

A *vertex deletion* causes a delete of all edges incident upon. Further, with this vertex as root, it cascades along the entire deleted out-neighborhood, up to L hops, potentially impacting a large neighborhood and being the most expensive of all update types. E.g., in Fig. 6(b), deletion of C would first lead to the removal of edges $C \rightarrow A$, $C \rightarrow D$, $E \rightarrow C$, and $B \rightarrow C$, and then the deletion of the vertex C itself. This is followed by an update propagation to A and D , since these were downstream from C , and so on.

Lastly, when a *vertex feature* is updated, the out-neighborhood that is affected is similar to vertex deletion, as updating the feature h_u^0 for vertex u impacts all its out-neighbors, and this impact cascades up to L hops. E.g., in Fig. 6(b), after the edge addition $C \rightarrow A$, if the features of vertex C change, it impacts its out-neighbors, A and D , and leads to a larger propagation downstream.

A key limitation of layer-wise recomputation is that updating the h_v^l embedding of vertex v at layer l requires us to fetch the embeddings for the previous layer h_u^{l-1} of *all its in-neighbors* u , regardless of whether their h^{l-1} embeddings were updated or not, as long as some of them were updated. *This leads to wasted computation because updating even a single in-neighbor among many requires aggregating the embeddings of all in-neighbors to compute the new embedding for the sink vertex, and this grows exponentially downstream.*

Next, we describe the incremental computation model of RIPPLE++ that avoids this by reducing the number of operations performed during aggregation to be proportional to the number of vertices updated.

3.3 Incremental Update Propagation in **RIPPLE++**

Incremental computation in **RIPPLE++** follows a similar initial step as **RC**. It *Applies* the graph updates that have been received onto the current graph (Fig. 11, Inset), and identifies the root vertices of these mutations. We start a BFS traversal from each *root vertex* of an update (§ 3.2) to identify downstream vertices affected at each hop, and whose embeddings need to be incrementally updated. This forms the *L-hop propagation tree*; leaves of this tree are the vertices whose predicted labels (h^3 embeddings) may be updated.

3.3.1 Operations on the Propagation Tree

We perform an iterative vertex-centric computation within the propagation tree, with vertices at distance l from the root vertex participating in *hop l* . This is similar to a *Bulk Synchronous Parallel (BSP)* model of execution [10, 31], with L iterative supersteps (hops) of execution. We employ a strictly *look-forward* computing model to propagate updates from a vertex through *message-passing*, with barrier-synchronization between hops.

In a superstep l , we perform several operations on each vertex at hop l as part of its lifecycle: *Compute*, *Prepare*, *Send* and *Aggregate* (Fig. 11, Inset). The vertex *computes* its updated embeddings (h^l) based on its current embeddings (h^{l-}) and the incoming messages from the previous hop, for $l > 0$. It then *prepares* the outgoing messages to be sent to its out-neighbors, and then *sends* these messages to the sink vertices. These messages carry incremental updates rather than the raw embeddings, as we describe later. This repeats until L hops are complete. Unlike sampling-based methods, all vertices in the propagation tree are updated to ensure deterministic behavior.

3.3.2 Inboxes in **RIPPLE++**

Each vertex maintains L logical *inboxes*, one for each hop at which it may be present from a root vertex being updated. Affected in-neighbors at hop $(l-1)$ of the propagation tree will place their incremental messages to this vertex in its *hop- l* inbox. The inbox will *aggregate* this message with other messages from other in-neighbors in this hop, and maintain just one aggregate message. E.g., in Fig. 6(c) A has 3 inboxes that are used to receive messages for its h^1 (from h^0 of C), h^2 (from h^1 of C) and h^3 (from h^2 of B, C, D), based on the level in the tree where A appears.

Messages in the inbox at hop l are processed by vertices after all vertices in the previous hop $(l-1)$ have completed their compute and send operations, consistent with the barrier in *BSP* [31, 49], which alternates between compute and communication phases. Such a “push” based approach, where only upstream vertices that are affected send messages to the inbox, avoids each vertex checking *all* its in-neighbors for any changes, as is done in a layer-wise recomputation approach.

3.3.3 Incremental Computation

An incremental message sent from a source vertex at hop l to its sink vertices at $(l+1)$ is meant to *nullify* the impact of the old embeddings (h^{l-}) of the source vertex and *include* the contribution of its current embeddings (h^l) on the sink vertices, thus forming a “delta”. Propagation of updates in **RIPPLE++** can happen due to different update conditions. We describe these, and their consequent actions, next using a *sum* aggregation function as an example.

The embedding of vertex u is updated from h_u^{l-} to h_u^l This can occur due to a direct update to the feature of vertex u (h_u^0 gets updated), or because u falls at hop $l < L$ of the propagation tree of another edge or vertex update. If u is not at the leaf of the tree, it will send a message m_{uv}^{l+1} to the $(l+1)$ inbox of its sink vertex v . The contents of m_{uv}^{l+1} are *prepared* such

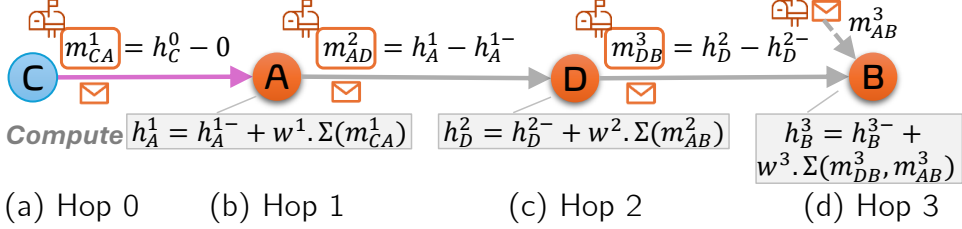


Figure 7: Messages (m_{edge}^{hop}) propagate from edge addition (C, A) to update the h^3 embedding of vertex B (Fig. 6), for a 3-layer GNN using *sum*. They negate the effect of the old embeddings ($h_A^{1-}, h_D^{2-}, h_B^{3-}$) to compute the new ones (h_A^1, h_D^2, h_B^3).

that they invalidate the effect of the old embedding h_u^{l-} on h_v^{l+1} and include the contribution from its new embedding h_u^l . For the *sum* operator this incremental message is $m_{uv}^{l+1} = h_u^l - h_u^{l-}$.

E.g., in Fig. 7(c), vertex D receives the incremental message $m_{AD}^2 = (h_A^1 - h_A^{1-})$ from A . When the update is applied to h_D^{2-} , it computes the new embedding by cancelling the terms, $h_D^2 = h_D^{2-} + w^2 \cdot m_{DA}^2 = h_D^{2-} + w^2 \cdot (h_A^1 - h_A^{1-}) = w^2 \cdot (h_C^1 + h_A^1)$, where $h_D^{2-} = w^2 \cdot (h_C^1 + h_A^{1-})$. This value of h_D^2 computed by our incremental approach with 1 *subtraction* and 1 *addition* is exactly what would have been computed by layer-wise recomputation, but using k *additions* over the embeddings from k in-neighbors.

An edge (u, v) was added/deleted to/from the graph Like the previous case, here again m_{uv}^{l+1} will nullify the effect of h_u^{l-} on h_v^{l+1} . But before the edge was added, the embedding h_v^{l+1} did not have any contribution from vertex u . So, this is a simplified variant of the previous case where we use a value of $h_u^{l-} = 0$ as the old embedding of u when preparing the incremental message (e.g., h_C^{0-} is used as 0 for m_{CA}^1 in Fig. 7(a)). Similarly, deleting an edge (u, v) means that v must not get any contribution from u , and hence we use $h_u^l = 0$ as the new embedding of u within m_{uv}^{l+1} .

Aggregation of message at the inbox Lastly, a vertex v can receive messages from multiple vertices at hop l . Due to the inherent *permutation-invariance* of the GNN aggregation functions due to their commutative property, the arriving messages can be aggregated in a vertex’s inbox in any order. For the *sum* operator, this aggregation is simply the sum of all incoming messages. In Fig. 7(d), besides m_{DB}^3 , vertex B also receives a message m_{AB}^3 from A due to an update of h_A^{2-} to h_A^2 . The messages that arrive at B ’s hop-3 inbox are *added* as they are received. The resultant h_B^3 is identical to the outcome if the updates had been applied individually.

Other linear aggregators This incremental computation model can easily be generalized to other linear aggregators beyond *sum*. For both *mean* and *weighted sum* each message is prepared such that it includes a *weight* α when propagated to a neighbor. The message to propagate a change from u to v at l hop is then modeled as $m_{uv}^{l+1} = \alpha h_u^l - \alpha h_u^{l-}$, where α is in-degree of the sink vertex for mean and the edge-weight for weighted sum, to effectively replace the effect of the old embedding with the new embedding of u at v . Similar to *sum*, message aggregation for linear accumulative messages is simple and just requires adding all incoming messages.

3.4 Generalization to Complex GNN Architectures

Till now, we have established the operation of the incremental model for linear aggregators; here, we extend it by identifying scenarios where complex aggregators, such as *min/max*, and attention-based (GAT), require recomputation, and introduce a hybrid incremental programming model used by **RIPPLE++** to support them.

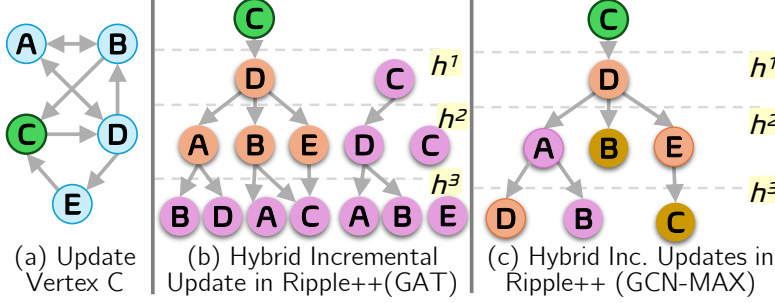


Figure 8: Propagation of updates in the *hybrid-incremental* model of RIPPLE++. Orange vertices are updated incrementally, purple are recomputed, and gold are unchanged for *max* operator.

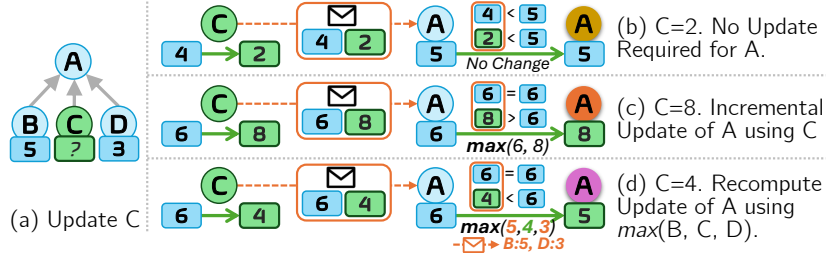


Figure 9: Propagating embeddings for a monotonic *max* agg.

3.4.1 Attention-based Architectures

Graph Attention Networks (GAT) [38], which introduces attention mechanisms into graph learning by assigning learnable importance weights to neighbors during aggregation, achieves more powerful learning than GCN. The embedding generated by the GAT layer for a vertex v at hop $l + 1$ is $h_v^{l+1} = \sum_{u \in \mathcal{N}_{in}(v)} \alpha_{uv}^l h_u^l$, where:

$$\alpha_{uv}^l = \frac{\exp(z_{uv}^l)}{\sum_{u \in \mathcal{N}_{in}(v)} \exp(z_{uv}^l)}, \quad z_{uv}^l = a^l \cdot (W^l h_u^l \| W^l h_v^l) \quad (3)$$

and a^l and W^l are learnable model parameters. Unlike other GNNs, GAT's hop- l coefficient for an edge (u, v) , α_{uv}^l , depends jointly on the h^l embeddings of both source and sink vertices (Eqn. 3). Also, changes to h_v^l will trigger changes to downstream embedding, h_v^{l+1} , and cause z_{uv}^l to be calculated for all $u \in \mathcal{N}_{in}(v)$, inevitably requiring access to all in-neighbors, which reduces to *recompute*. But, for out-neighbors of v at hop- $(l + 1)$ that have *not yet been updated*, the embeddings can be updated *incrementally*.

In Fig. 8, the GAT embedding for layer $(l + 1)$ of vertex D is $h_D^{l+1} = (\alpha_{AD}^l h_A^l + \alpha_{CD}^l h_C^l)$. The coefficients α_{uD}^l , for all $u \in \{A, C\}$, are computed using Eqn. 3. When simplified, $h_D^{l+1} = \frac{\sum_u \exp(z_{uD}^l) h_u^l}{\sum_u \exp(z_{uD}^l)}$. Due to an update from h_C^0 to h_C^0 , the only parts of h_D^1 affected are $\exp(z_{CD}^0) h_C^0$ in the numerator and $\exp(z_{CD}^0)$ in the denominator. So, the incremental message sent to any vertex will have two parts: numerator and denominator. E.g., C prepares the message: $m_{CD}^1 = \langle (\exp(z_{CD}^0) h_C^0 - \exp(z_{CD}^0) h_C^0), (\exp(z_{CD}^0) - \exp(z_{CD}^0)) \rangle$.

We propose a *hybrid-incremental* approach for GAT. Any vertex u that appears at hop l of the propagation tree performs *recomputation* from hop $(l + 1)$ onward (Fig 8(b), *purple* vertices). For vertices that have not been updated yet in the tree, we use *incremental* (*orange*).

3.4.2 Monotonic Aggregation Functions

Monotonic aggregators like *max* and *min*, unlike their accumulative counterparts, cannot be updated through local deltas since the effect of an update is apparent only when it reaches the

current hop (Fig. 9). They require recomputation if an update invalidates the current extrema’s contribution, but can be done incrementally if the update retains it, as we discuss next.

RIPPLE++ extends the above hybrid-incremental approach to GNNs with monotonic aggregation functions. A message sent from vertex u to v (m_{uv}^{l+1}) at hop $l+1$ contains both the old and the new l -hop embedding of the vertex u , h_u^{l-} and h_u^l . When vertex v receives a message $m_{uv}^{l+1} = \langle h_u^{l-}, h_u^l \rangle$, it can take one of three actions, illustrated in Fig. 9 using \max .

No update is computed for v In the trivial case, where the new embedding h_u^l is identical to the current embedding of v , an update is not needed. Importantly, if the old embedding h_u^{l-} did not contribute to the current embedding of v , and the new embedding h_u^l does not contribute either, the update from u is irrelevant to v and no change is performed at v . No further propagation is required. E.g., in Fig 9(b), the current embedding of A did not have any contribution from the old embedding of C (value 4) before the update, and will not be impacted by the update to C (value 2) either. Here, the embedding at A remains unchanged at 5 (gold color), and A does not propagate changes further.

Incremental update is computed at v The new embedding h_u^l is greater than the current embedding at v . In this case, v incrementally updates its embedding by replacing the old contribution from u with the new one, avoiding a full recomputation. E.g., in Fig. 9(c), the current embedding of A included a contribution from the old embedding of C (value 6), and the updated value from C (value 8) can cover the previous value. Hence, the new embedding of A (e.g., 8) can be computed incrementally.

Recompute performed at v The old embedding h_u^{l-} , contributed to the current embedding of v , but the new embedding h_u^l no longer preserves the monotonic consistency required for performing an incremental update, e.g., with a \max aggregator, the new value may no longer be the maximum among all neighbors. Here, v must recompute its embedding from all current contributors to ensure correctness. In Fig. 9(d), the old embedding of C (value 6) was the highest among the neighbors of A , but the updated embedding (value 4) is no longer the maximum. Hence, A recomputes its embedding by taking the new maximum from among all its neighbors (5, from B), resulting in its new value of 5. This change is propagated as needed.

RIPPLE++ splits the active vertices at each hop into three sets matching these scenarios for processing – vertices that do not need updates (*gold* in Fig. 8(c)) are left unchanged and do not propagate further; vertices that need recomputation (*purple*) pull the embeddings of all their in-neighbors; and vertices that are updated incrementally (*orange*) apply the message to get the new embedding.

3.5 Analytical Modeling of RIPPLE++ Benefits over RC

Next, we analytically examine the advantages of RIPPLE++ over layer-wise recomputation (**RC**). Let a_l denote the number of active vertices at hop- l of the propagation tree, i.e., vertices whose h^l embeddings require updating. Let δ be the average degree of the graph and d_l be the dimensionality of the embedding at hop- l . For simplicity, we assume a *sum* aggregation function in this analysis.

In RC, updating the embeddings of a_l active vertices at hop- l involves two primary steps.

1. *Aggregate in-neighbors*: Here, the h^{l-1} embeddings of the in-neighbors of each active vertex are aggregated, requiring $(a_l \cdot \delta \cdot d_{l-1})$ floating-point (FP) operations.
2. *Compute*: Here, the aggregated embeddings of size $a_l \times d_{l-1}$ are multiplied with the weight matrix of size $d_{l-1} \times d_l$, incurring $(a_l \cdot d_{l-1} \cdot d_l)$ FP operations.

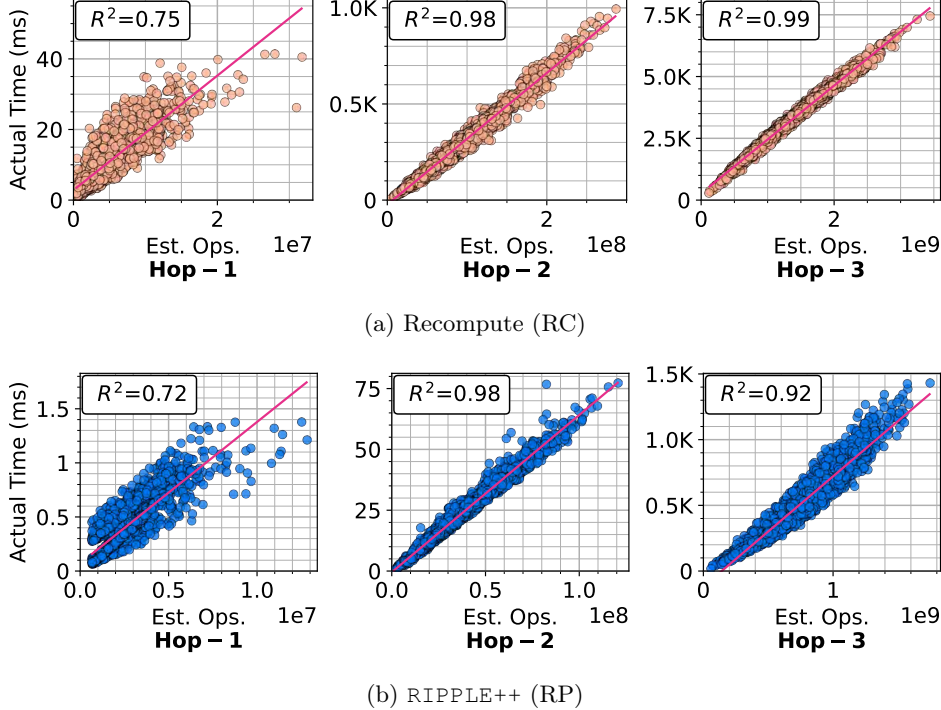


Figure 10: Benefits analysis of RIPPLE++ over **RC** for inferencing a 3-layer GC-S for Products graph with $bs = 100$.

Thus, the total estimated cost of RC to process vertices at hop- l is $(a_l \cdot \delta \cdot d_{l-1} + a_l \cdot d_{l-1} \cdot d_l)$.

Conversely, in RIPPLE++, updating the embeddings of a_l active vertices at hop- l involves two primary steps.

1. *Prepare and aggregate message*: Here, messages are generated for the active vertices in hop $(l-1)$, with each of the a_{l-1} active vertices sending a message to its out-neighbors and they aggregating it in their inbox. This requires $(a_{l-1} \cdot d_{l-1} + a_{l-1} \cdot \delta \cdot d_{l-1})$ FP operations.
2. *Compute*: Here, the aggregate messages are used to compute the embeddings for hop- l by multiplying them by the weight matrix and adding the result to the current embedding, costing $a_l \cdot d_{l-1} \cdot d_l + a_l \cdot d_l$ FP operations.

The total estimated compute cost for RIPPLE++ to process a_l vertices at hop- l is $(a_{l-1} \cdot \delta \cdot d_{l-1} + a_{l-1} \cdot d_{l-1} + a_l \cdot d_{l-1} \cdot d_l + a_l \cdot d_l)$, which can further be approximated down to $(a_{l-1} \cdot \delta \cdot d_{l-1} + a_l \cdot d_{l-1} \cdot d_l)$.

Thus, RC requires $\approx (a_l \cdot \delta \cdot d_{l-1} + a_l \cdot d_{l-1} \cdot d_l)$ FP operations at hop l , whereas RIPPLE++ requires $\approx (a_{l-1} \cdot \delta \cdot d_{l-1} + a_l \cdot d_{l-1} \cdot d_l)$ FP operations. Since the active vertices can only expand or remain constant ($a_l \geq a_{l-1}$), the difference in cost simplifies to $(a_{l-1} - a_l) \cdot \delta \cdot d_{l-1}$. Hence, RIPPLE++ is strictly cheaper when the frontier expands ($a_l > a_{l-1}$), and the two methods have identical costs when the frontier size remains unchanged ($a_l = a_{l-1}$). RIPPLE++ never exceeds RC's cost.

Fig. 10 shows a strong correlation between the estimated FP operations and the actual execution time for both RC (Fig. 10a) and RIPPLE++ (Fig. 10b) for GC-S inferencing on the Products graph (see § 6.1 for experiment setup). The correlation is particularly strong at hop-2 and hop-3 ($R^2 \geq 0.92$), which dominate the total inference time, confirming that our FP count model can reliably predict runtime. Hop-1 exhibits a weaker correlation ($R^2 \approx 0.72$ – 0.75) due to fixed-cost overheads, which are more prominent at small workloads. These are, however, very small in absolute times (< 50ms) compared to 1000s of ms taken by hops 2 and above.

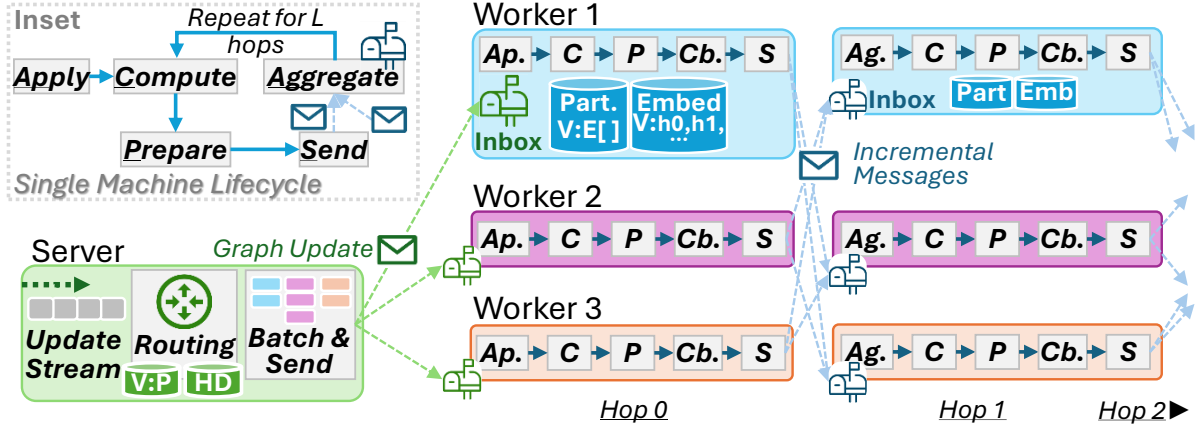


Figure 11: Distributed Architecture of RIPPLE++. Top-left *Inset* shows single machine lifecycle.

4 Distributed GNN Inference in RIPPLE++

Real-world graphs can be large in size. Besides the graph structure and features, we also need to store the various embeddings for all vertices to help with the incremental computation. These data structures can be memory-intensive, exceeding the RAM of a single machine, e.g., for Papers, 26GiB is used for the graph structure (111M vertices, 1.6B edges), 56GiB for features, and 132GiB for intermediate embeddings created when computing a 3-layer GNN (> 200 GiB in total). We design a distributed execution model for RIPPLE++ (Fig. 11) to perform incremental computation over updates received for the graph partitioned across machines in a cluster, while retaining an execution flow similar to a single-machine (Fig. 6).

4.1 Partitioning the Graph

We consider a typical scenario where the initial part of the graph has arrived, and the updates start streaming in. This initial graph structure, features, and their embeddings computed for the GNN are partitioned and kept in-memory on *worker* machines [7, 28, 35, 51, 52]. We use METIS [21] to partition the initial graph so that the vertex count is balanced across workers (balances compute load), and edge-cuts across partitions are minimized (reduces network communication), with one partition per worker. We replicate the boundary (“halo”) vertices having edge cuts to reduce communication during BFS propagation [52].

4.2 Server-Worker Execution Model

We adopt a worker–server architecture for distributed execution (Fig. 11). The *server* receives the incoming stream of events and routes them to the relevant workers. The server also maintains metadata about the workers, e.g., vertex to partition mapping (V:P), high-degree vertices (HE), for efficient routing.

Each *worker* stores the embeddings for its local vertices, and is responsible for executing the lifecycle for its local vertices (Fig. 11): receive messages, update embeddings, and prepare and send incremental messages. Unlike a single-machine setup where all vertices have inboxes, doing so for large graphs is memory-intensive and unnecessary since only a subset of vertices participate in the propagation tree. Instead, each worker maintains a *managed inbox pool* that gets *assigned* to vertices on-demand, when a message is received. After processing a batch, the inboxes are unassigned and can be reassigned to other active vertices in the future. We dynamically expand this allocation pool on-demand. This reduces memory overhead from repeated allocation and right-sizes memory use.

Workers do not hold embeddings for *halo vertices*, but maintain inboxes for them. These serve as a proxy for sending messages from local to halo vertices in a partition, and aggregate

Algorithm 1 Locality-aware Routing and Vertex Placement

```
1: procedure ASSIGNEDGE(Edge  $v_{12}$ , Partitions  $P_i$ )
2:    $\pi(v)$ : Partition assigned to vertex  $v$ 
3:    $\text{load}(P_i)$ : Number of vertices assigned to partition  $P_i$ 
4:    $H(v)$ : Lookup function, returns True if  $v$  is a high in-degree vertex, False otherwise
5:   if  $v_1, v_2$  exist then
6:     if  $\pi(v_1) = \pi(v_2)$  then  $\pi(v_{12}) \leftarrow \pi(v_1)$ 
7:     else CUTEDGE( $\pi(v_1), \pi(v_2)$ )
8:     end if
9:   else if  $v_2$  exists then
10:    if  $H(v_2)$  then  $\pi(v_{12}) \leftarrow \pi(v_2)$ 
11:    else  $\pi(v_{12}) \leftarrow \arg \min_i \{\text{load}(P_i)\}$ 
12:    end if
13:   else  $\pi(v_{12}) \leftarrow \arg \min_i \{\text{load}(P_i)\}$ 
14:   end if
15: end procedure
```

local partition messages using a MapReduce-style *combiner (Cb.)* (Fig. 11) [31]. After the *local send* operation in a hop, we perform a *remote send* of these aggregate messages to remote workers having their partition. We perform another receiver-side aggregation, and start the next hop’s compute.

4.3 Request Batching and Routing

The server receives a stream of both vertex-level and edge-level updates that are routed to appropriate workers. The server creates *batches* of updates destined for each worker, of size of bs (Fig. 11). Both *edge updates* are of the form v_{12} , which indicates an edge from vertex v_1 to vertex v_2 . We model vertex *additions* also as an edge update as we assume that at least one edge will be added along with a new vertex. *Vertex deletions* and *feature updates* apply only to vertices already present in the graph.

A vertex update/delete is easy to route, and is assigned to the worker (partition) having it as a local vertex. The server maintains a *Vertex-Partition map (VP)* from each vertex to its partition. But edge additions or deletions may span workers.

- An edge request is completely local to a worker if both the incident vertices of an edge update are local to the partition. Here, the update is assigned to that worker.
- An edge request spans workers if its source and sink vertices are local to different partitions. We assign the edge update to the worker that has the source vertex (or hop-0) of the edge update. We also send a *no-compute* request to the sink vertex’s worker to update its partition with the new edge.

Finally, vertex addition requires more sophisticated handling since it must assign the new vertex to a partition while considering placement quality for load balancing and minimizing edge cuts, similar to graph partitioning. RIPPLE++ allows users to configure custom routing algorithms, and we propose two: (1) A simple *hash-based routing*, where the new vertex is assigned to a partition based on hashing its vertex ID onto a partition ($V \% P$); and (2) A *locality-aware routing*, discussed next, that minimizes edge cuts while balancing load across partitions. Once bs streaming updates for a batch have arrived in total, the server sends them to the respective workers.

4.4 Locality-aware Routing for Updates

We design a locality-aware routing strategy for edge-events, inspired by our prior work [6]. Alg. 1 running on the server decides which partition to place an incoming edge v_{12} , caused by an edge addition/deletion or vertex addition as part of a new edge.

- If both incident vertices v_1 and v_2 already exist in partitions, this is either an edge addition or deletion (line 5). Here, if v_1 and v_2 are on the same partition (line 6), edge v_{12} is sent to that partition, avoiding inter-worker communication.
- If the incident vertices are on different partitions, a cut-edge is introduced between partitions $\pi(v_1)$ and $\pi(v_2)$ (line 7). This routes the edge to the source vertex partition but sends a copy to the other partition to update the graph.
- If only one vertex exists, v_2 , then the other vertex v_1 is new, and indicates a vertex addition (line 9). We consider if the incident vertices of v_{12} have a *high in-degree* – co-locating the edge with the vertex with a high degree enhances locality and reduces the inter-worker communication for the propagation tree. We maintain a *High in-Degree set (HD)* at the server for this. If the existing vertex v_2 is part of the HD set, v_{12} is placed on its partition (line 10). Else, we place the edge on the partition with the least load in an effort to *balance* the vertex load across partitions (line 11).
- If neither vertex exists (line 11), the edge is assigned to the least-loaded partition, again to balance the vertex load.

The HD set (Fig. 11) has vertices with degree greater than *twice the current average degree* of the graph, and is refreshed to reflect structural changes, e.g., after each 0.5M updates. Hash-based routing has constant *time and space complexity*. Locality-based routing also has constant-time lookups, but incurs $\mathcal{O}(V)$ time to refresh the HD set. It also uses $\mathcal{O}(V)$ space to track vertex membership and HD nodes. Overall, this strategy ensures that we systematically minimize communication, maintain load balancing, while ensuring rapid routing of streaming updates in large distributed graphs.

4.5 Update Processing

Upon receiving a batch of updates, a worker applies the topology and feature changes to its local partition and embeddings (*Apply* in Fig. 11). Depending on the update, it prepares messages for the hop-1 vertices (*Prepare*). For local vertices, the message handling is similar to a single-machine execution. But for halo vertices, the messages are *combined* (*Cb.*) in a local mailbox for the halo, across all propagation trees at hop-0. Once all the vertices in this hop are processed by the worker, the combined messages are sent to matching vertices on remote workers, before the next hop starts.

For subsequent hops, $l \in [1, L]$, the workers aggregate the messages in the vertex inboxes, compute the local embeddings, and prepare downstream messages, similar to a single machine; as before, local messages are delivered and aggregated immediately, while remote messages are combined and sent to the remote inbox after the hop completes. We leverage MPI for efficient message passing between workers. The next hop starts only after embeddings in the prior hop are updated, and incremental messages are delivered to all workers. This repeats L times till we get the final layer embeddings for the batch.

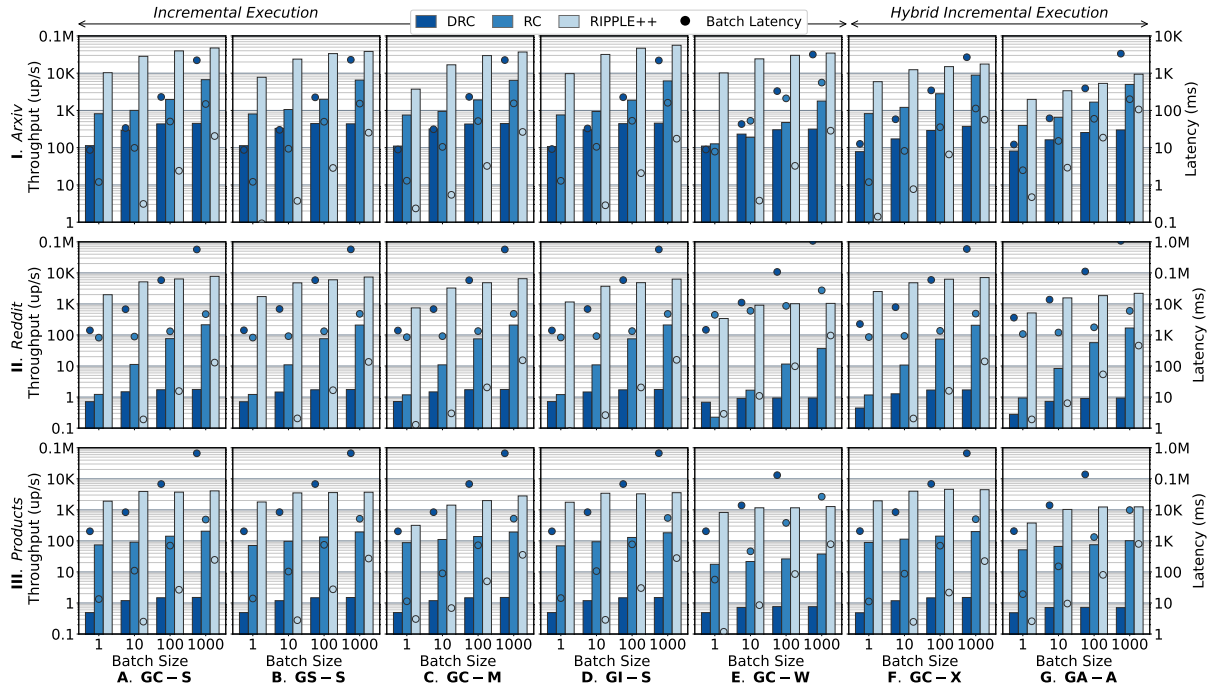


Figure 12: Single machine performance of RIPPLE++ against DRC and RC on the 2-layer variants of 7 GNN workloads for Arxiv, Reddit, and Products across bs . Left y-axis shows *Throughput* (updates/second, bar, log scale) while right y-axis has *mean batch latency* (milliseconds, marker, log scale)

5 RIPPLE++ Implementation and Baselines

RIPPLE++ is implemented natively in Python for both single-machine and distributed setups using NumPy v2.0, and is open-sourced ². The distributed setup utilizes MPI for inter-process communication. We only support CPU-based execution due to its competitive performance relative to GPU, as discussed later. We also implement the *vertex-wise* and *layer-wise recompute* inference strategies as baselines using the SOTA DGL v1.9 framework with a PyTorch backend [41]. We natively implement the *layer-wise recompute* strategy directly using Python, due to the high overheads for graph updates using DGL. We also compare RIPPLE++ against InkStream [42], a SOTA streaming GNN inference framework.

To maintain a fair comparison, all strategies update only the embeddings of impacted vertices at the final hop when performing a batch of updates. We consider the whole neighborhood of a vertex at each hop during inference, without sampling or any approximations, to ensure that the resulting predictions are accurate and deterministic. Finally, we confirm that RIPPLE++ calculates *accurate* embeddings at all hops of inferencing, within the limits of floating-point precision.

6 Experimental Evaluation

We evaluate RIPPLE++ on diverse graph datasets and GNN workloads for single-machine and distributed setups, and compare it against contemporary baselines.

Table 2: Graph datasets used in experiments.

Graph	V	E	# Features	# Classes	Avg.	In-Deg.
<i>Arxiv</i> [18]	169K	1.2M	128	40	6.9	
<i>Reddit</i> [17]	233K	114.9M	602	41	492	
<i>Products</i> [18]	2.5M	123.7M	100	47	50.5	
<i>Papers</i> [18]	111M	1.62B	128	172	14.5	

6.1 Experimental Setup

6.1.1 GNN Workloads

We evaluate four popular GNN models for vertex classification: *GraphConv* [23], *GraphSAGE* [17], *GINConv* [45], and *GATConv* [38]. These are paired with common aggregations: linear (sum, mean, weighted sum), monotonic (max, min), and attention-based, to construct seven representative workloads: GraphConv with Sum (**GC-S**), GraphSAGE with Sum (**GS-S**), GraphConv with Mean (**GC-M**), GINConv with Sum (**GI-S**), GraphConv with Weighted Sum (**GC-W**), GraphConv with MaX (**GC-X**), and GATConv with Attention (**GA-A**).

6.1.2 Datasets

We use 4 well-known graph datasets for our evaluation (Table 2): ogbn-arxiv (*Arxiv*), a citation network [18]; *Reddit*, a social network [17]; ogbn-products (*Products*), an e-commerce network [18]; and a large citation network, ogbn-papers100M (*Papers*) [18], which does not fit in the memory of a single machine and is used only for distributed execution. We remove a random 20% of vertices and edges from each graph, and the remaining 80% of vertices and edges serve as the initial graph snapshot to which streaming updates arrive. We train the GNN models on these 80% snapshots and extract the embeddings, which form the initial state for inference. In the distributed setup, we partition the graph using METIS [21] into the required number of parts and load the local subgraph, their embeddings, and the halo vertices in memory.

We generate a stream of events comprising the five types of updates using the probability distribution of these update types from the Facebook workload ³. For the single-machine experiments, we generate 200K update events for Arxiv, and 20M events each for Products and Reddit, while for distributed experiments on Papers, we generate 5M events. Importantly, given the Facebook distribution of update types, with additions exceeding deletions, the graph size never decreases as events are applied; it either grows or remains unchanged.

6.1.3 Hardware Setup

All single-machine experiments are conducted on workstations with 12-core AMD Ryzen 9 7900X processor (4.7GHz) with 128 GiB of RAM. The distributed execution is performed on a cluster of 24 compute servers, each equipped with a 16-core Intel Xeon Gold CPU (2.9GHz) with 128 GiB of RAM, and connected over 10 Gbps Ethernet. We also briefly compare the DGL implementation of vertex-wise and layer-wise recompute using both CPU and GPU to demonstrate that the GPU-based execution is occasionally slower than the CPU-based execution, and that both DGL variants are slower than our custom implementation of layer-wise recompute on the CPU. For this, we use the same workstation as above with an NVIDIA RTX 4090 GPU card with 24 GiB GPU memory.

To ensure fair comparison, we benchmark our implementations of DGL’s vertex-wise inference on the CPU (**DNC**) and CPU+GPU (**DNG**), with its layer-wise recompute strategy on

²<https://github.com/dream-lab/ripple>

³<https://github.com/facebookarchive/linkbench/blob/master/config/FBWorkload.properties>

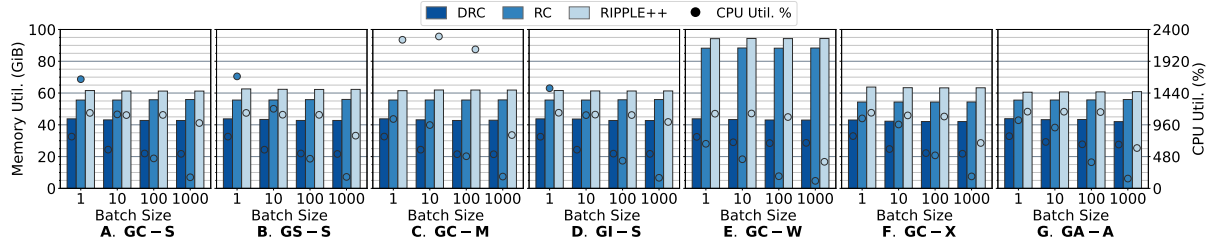


Figure 13: Single-machine systems utilization of RIPPLE++ against DRC and RC on the 2-layer variants of 7 GNN workloads on Products. Left y-axis shows *Memory Utilization* (GiB, bar) while right y-axis has *CPU Utilization* (%), marker)

the CPU (**DRC**) and CPU+GPU (**DRG**). We show that **DRC** and **RC** running on the CPU act as the most competitive baselines to compare against RIPPLE++’s incremental approach. For brevity, we report this experimental comparison in the Appendix 9.1.

6.2 Single-Machine Performance

6.2.1 Comparison With Baselines

We contrast the single-machine performance of RIPPLE++ (RP) with the DRC and RC baselines, for Arxiv, Reddit, and Products graphs, for the 7 GNN workloads using different bs . All experiments are run for a maximum of 4 hours or till all events are exhausted. Fig. 12 shows the *throughput* (bar, left y-axis) and *batch latency* (marker, right y-axis), for the three graphs shown in three rows, and similarly Fig. 13 plots their *memory* (bar, left y-axis) and *CPU utilization* (marker, right y-axis). For the first 5 workloads (GC-S, GS-S, GC-M, GI-S, and GC-W) in Figs. 12 and 13 (A-E), RIPPLE++ performs *purely incremental* processing, while for GC-X and GA-A (F and G), a *hybrid incremental* approach is required.

Arxiv RIPPLE++ (RP) achieves a maximum speedup of $\approx 128\times$ over RC and $\approx 124\times$ over DRC (Fig. 12, first row). The maximum absolute throughput achieved by RP exceeds 56K up/s for $bs = 1000$ for GI-S (bar, left y-axis) with latencies between 0.06–104 ms per batch (bar, left y-axis), across all bs and GNNs. As expected, the absolute throughput values averaged across all 7 workloads increase from ≈ 8 K up/s to ≈ 35 K up/s as bs increases from 1 to 1000, since larger batches allow for more efficient amortization of per-batch overheads and hence higher throughput. However, this comes at the cost of higher batch latencies. This offers an opportunity to trade-off throughput and latency according to application requirements.

Reddit For Reddit (Fig. 12, second row), increasing bs from 1 to 1000 leads to an average throughput increase across all workloads, from about ≈ 1.3 K up/s to ≈ 5.5 K up/s. RP achieves a maximum speedup for GC-S of $1628\times$ over RC for $bs = 1$ and $4393\times$ over DRC for $bs = 1000$, with a peak of ≈ 7.8 K up/s seen for GC-S at $bs = 1000$. Batch latencies range from 0.3–960 ms across all bs and GNNs.

Products For Products (Fig. 12, third row), RP achieves a peak speedup for workload GC-S of $\approx 45\times$ over RC for $bs = 10$ and $3800\times$ over DRC for $bs = 1$. The maximum throughput reaches ≈ 4.5 K up/s at $bs = 1000$ for workload GC-X, with latencies of 0.5–800 ms. On average, throughput across all seven GNNs increases from roughly 1.3K up/s to ≈ 3 K up/s as the bs grows from 1 to 1000, with a corresponding rise in batch latencies.

Overall, RIPPLE++ offers throughput up to 56K up/s with latencies of 0.06–960 ms, that translate to a throughput speedup 20–438 \times over RC and 75–2771 \times over DRC, averaged over

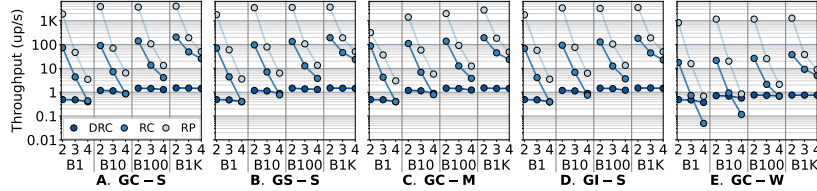


Figure 14: Single machine *Throughput* (log scale) of RIPPLE++ (RP) against DRC and RC on the 2-, 3-, and 4-layer variants of 5 GNN workloads for *Products*, across bs .

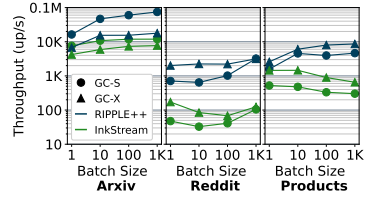


Figure 15: Throughput of RIPPLE++ and InkStream for 2-layer GC-S and GC-X.

datasets, GNNs, and batch sizes, thus making it compelling for real-time GNN inferencing applications.

6.2.2 Performance Drill-down on Single-Machine

Next, we dive deeper into the performance of RIPPLE++ on a single-machine setup and make the following key observations.

Increasing bs gives minimal performance benefits for DRC As the bs increases from 1–1000, throughput values increase only by about $\approx 3.9\times$ for Arxiv and $\approx 2.6\times$ for Reddit and Products on average for DRC, with the increase between 100 to 1000 being a meager 8% for Arxiv and $\approx 2\%$ for Reddit and Products (Fig. 12). As we see in Fig. 19 of Appendix, a significant portion of the total batch processing time is spent applying updates to the DGL graph itself (*Update* in Fig. 19). As the bs increases, the overhead of modifying the graph grows proportionally and begins to dominate the end-to-end batch time, thus diminishing the relative benefit of batching for the actual embedding propagation.

GC-W has a lower performance compared to other purely incremental GNN workloads, GC-S, GS-S, GC-M, and GI-S GC-W for $bs = 1000$ achieves a throughput on RP of $\approx 34K$, $\approx 1.1K$, and $\approx 1.3K$ up/s for Arxiv, Reddit, and Products, respectively, in contrast to $\approx 45K$, $\approx 7K$, $\approx 3.5K$ up/s achieved for GC-S – GI-S, indicating an average drop of $\approx 57.4\%$, from Fig. 12. RC also sees a similar average drop of 78% for GC-W, across graphs, and similarly for DRC. This is due to the additional *weighted aggregation* required in GC-W. Unlike simpler aggregation functions such as *sum* or *mean*, which combine neighbor embeddings directly, weighted aggregation introduces an extra computational step – each neighbor embedding must first be multiplied by its associated edge-weight before aggregation, significantly increasing the compute overhead. Notably, the weights fetching and multiplication are non-natively vectorized operations, causing a drop in CPU% (Fig. 13, *marker, right y-axis*) for $bs = 1000$, from $\approx 880\%$ for the other incremental GNNs to $\approx 420\%$ for GC-W; hence, the compute takes longer.

The throughput speedup of RP over RC decreases as the bs increases As the bs increases from 10 to 1000, the average speedup of RP over RC across all 7 workloads drops from approximately $35\times$ to only $7\times$ for Arxiv, $388\times$ to $30\times$ for Reddit, and $33\times$ to $20\times$ for Products. As discussed in § 3.5, the relative advantage of RP over RC diminishes when a_{l-1} approaches a_l . This occurs because as bs increases, it causes a_{l-1} to cover a larger part of the graph with greater overlap between vertex neighbors, leaving less headroom for a_l to grow, which reduces the relative throughput benefits.

Hybrid incremental RP for GA-A is worse than its purely incremental counterparts RP employs a hybrid incremental approach for GA-A due to the unique requirements of the GAT architecture, i.e., once a vertex is seen in the propagation tree at hop- l , its embeddings for

layers deeper than l have to be recomputed (§ 3.4.1). As expected, we notice a significant drop in throughput for GA-A as compared to other GNNs (Fig. 12, last column). E.g., with $bs = 1000$, RP attains a maximum throughput of $\approx 9.4K$, $\approx 2.2K$, and $\approx 1.25K$ up/s on Arxiv, Reddit, and Products, respectively. In contrast, the maximum throughput for purely incremental workloads, GC-S – GI-S, reaches $\approx 56K$, $\approx 7.8K$, and $\approx 4K$ up/s.

Hybrid incremental RP for GC-X performs relatively well despite its hybrid nature GC-X also uses a hybrid incremental like GA-A, but its performance on RP is competitive with purely incremental GNNs. Despite using a hybrid approach, GC-X uses the *max* function that offers a unique opportunity to prune the path of the propagation tree if a vertex’s embeddings do not change. Hence, GC-X either outperforms on Products (by 1.1–3.4 \times) or matches for Reddit the throughput of purely incremental GNNs using RP, for $bs = 1000$. But its throughput on Arxiv drops to $\approx 17.6K$ up/s, compared to 37K–56K up/s for the incremental models, since the fraction of active vertices at the final hop that require recomputation (§ 3.4.2 and Fig. 9(b)), is substantially higher for Arxiv ($\approx 47\%$) than for Reddit ($\approx 25\%$) or Products ($\approx 8\%$). This increased recomputation rate significantly reduces the throughput for Arxiv.

The memory usage of RP is higher than the baselines, RC and DRC Fig. 13 reports the memory utilization of the different approaches. We see a noticeable increase in the memory usage of both RP and RC than DRC, increasing from ≈ 43 GiB for DRC to ≈ 60 GiB for RC and ≈ 66 GiB for RP, averaged across bs and GNNs. This is due to how the graph structures are stored. While the embeddings stored in memory remain the same across the three strategies, the graph topology for DRC is stored as sparse matrices, which have a smaller memory footprint than our edge list. We also see a $\approx 10\%$ uptick in RP’s memory than RC due to the extra data structures to store the intermediate messages (§ 3.3). Lastly, we note a significant increase in the memory usage for RC and RP for GC-W (94 GiB for GC-W vs. ≈ 62 GiB on average for the others). This is expected since GC-W requires RP and PC to explicitly store the edge weights in a separate data structure, as compared to DRC, where the edge weights are merged into the sparse matrix representations for the graph topology. While RP incurs higher memory usage, this offers a significant reduction in compute time and substantial speedup in throughput, e.g., up to 128 \times over RC for Arxiv. If memory is a limiting factor, RP can operate in a distributed setup, albeit with some performance trade-offs.

6.2.3 Scaling with Number of GNN Layers

Next, we examined the impact on performance as the number of layers in the GNN models varies. Fig. 14 shows the throughput of RIPPLE++ (RP), DRC and RC with 2–4 layers. GNN models rarely exceed 4 layers. The increase in depth exponentially increases the size of each propagation tree, and can eventually encompass the whole graph.

RP sees a drop from $\approx 3.1K$ up/s to 41 up/s as the layers increase from 2 to 4 for $bs = 1000$. This reflects the number of affected vertices growing rapidly with the model depth, and the time taken to propagate these changes. The respective drop in RC is from 162 up/s to 20 up/s while DRC maintains the throughput at ≈ 1.3 up/s. This is because the time to process a batch by DRC is dominated by the *topology update* (e.g., taking $\approx 80\%$ for $bs = 10$ for Products in Fig. 19b), which is unaffected as the number of layers increases (Appendix 9.1). Hence, the throughput shows negligible change in DRC with more GNN layers; at the same time, the throughput is too low to begin with, due to the topology update costs.

For GC-W, the throughput for RC drop below that of DRC as the number of layers increases: 0.33 up/s vs. 0.4 up/s for $bs = 1$, and 0.66 up/s vs. 0.83 up/s for $bs = 10$. The edge list used by RC for the topology takes more time to collect the edge weights, which are maintained separately, for smaller batch sizes. As the update time for DRC increases for larger $bs \geq 100$ due to its CSR format, RC resumes outperforming DRC.

Lastly, the throughput of RP approaches RC for larger $bs = 100$ and $bs = 1000$ with 4 layers. As discussed, increasing the model depth causes a_{l-1} to approach a_l since a_{l-1} (for larger l) will cover a larger fraction of the graph with significant overlap in the out-neighbors (§ 3.5), leading to diminished benefits from incremental processing.

6.2.4 Comparison with InkStream

InkStream⁴ [42] is a recent SOTA work that is closest to us, as it too adopts an incremental inference approach to reduce redundant recomputation. We first discuss the design limitations of InkStream and then report an experimental comparison of RIPPLE++ against it.

Limitations of InkStream Despite offering incremental inferencing like us, InkStream suffers from several fundamental design limitations that restrict its scalability and applicability in real-world settings. It assumes that all updates are known *a priori*, i.e., even the ones that will arrive in the future, and processes them as a single batch. To allow comparison in a streaming setting, we had to extend InkStream with new data structures that preserve the graph state across batches and invoked it iteratively. Further, InkStream does not support attention-based models like GAT, and is limited to only edge additions and deletions. Finally, InkStream lacks a distributed execution model and is limited to the memory on a single machine, e.g., preventing it from running our *Papers* experiment.

Performance Comparison To enable a fair comparison with InkStream (IS), we generate a trace with equal number of just edge additions and deletions starting with the 80% graph, resulting in 400K events for Arxiv and 40M events for Reddit and Products. As before, experiments ran for the earlier among 4 hours or till all updates are processed.

Fig. 15 compares the relative performance of RP and IS on two 2-layer workloads, one purely incremental (GC-S) and one hybrid incremental (GC-X), evaluated for 4 batch sizes. Across all datasets and workloads, RP achieves markedly higher throughput than IS. On Arxiv for $bs = 1000$ with GC-S, it reaches up to 74.5K up/s compared to just 12K up/s for IS, and with GC-X, 17.8K up/s on RP against 7.7K up/s for IS, with average speedups of 4.4 \times and 2.2 \times across all batch sizes. On Reddit, RP offers 22.5 \times throughput improvement over IS for GC-S and 24.0 \times for GC-X, while for Products, RP is 9.9 \times and 7.0 \times faster than IS for these GNNs

This performance gap is due to IS’s inefficient data handling that is based on Python’s native *list* and *defaultdict* within its *EventQueue* for message handling, and employs dictionaries of lists to represent the graph topology. This design imposes an iterative, per-element processing model. In contrast, RP employs NumPy arrays for bookkeeping (e.g., for *messages*, *embeddings*), which enables efficient vectorized computation. Further, RP also supports additional aggregation operators and models like GAT, and also offers distributed execution.

6.3 Distributed Performance

The distributed experiments are performed on the Papers dataset and run for a minimum of 8 hours, or till 5M updates are processed. Each partition runs on an exclusive machine, with the server running on a separate node. For brevity, we report results for 3 of the 7 GNN workloads. We compare the performance of distributed RIPPLE++ (RP) against a distributed model of recompute that we implement (RC). As mentioned, distributed DGL (DistDGL) [52] does not support online graph updates, while InkStream does not support distributed execution.

⁴<https://github.com/WuDan0399/InkStream>

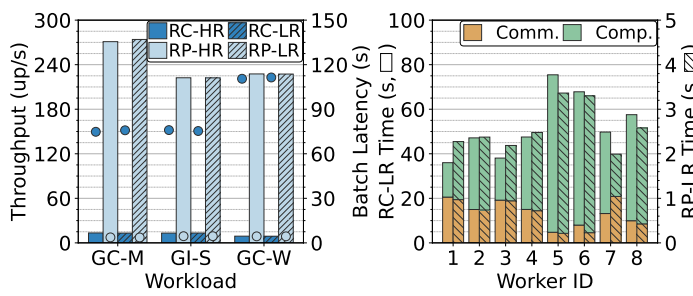


Figure 16: Distributed performance of RP and RC on 3-layer GNNs for Papers, $bs = 1000$ and 8 partitions.

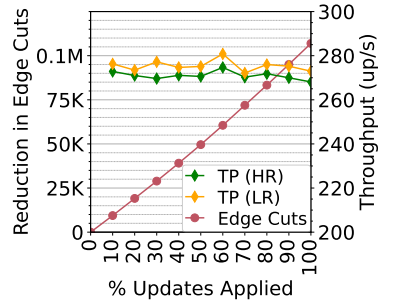


Figure 17: Drop in edge cuts of LR vs. HR; 8 parts, Papers, GC-M.

6.3.1 Comparison With Baseline

Fig. 16 shows the throughput for GC-M, GI-S, and GC-W on Papers for 8 partitions and $bs = 1000$. RP with the hash routing achieves $20.3\times$, $16.9\times$ and $25.2\times$ faster throughput than RC for GC-M, GI-S, and GC-W, respectively (Fig. 16, left subfigure, solid bar); this improvement is $20.8\times$, $16.7\times$, and $25.3\times$ using the locality-aware (hatched bar). This confirms that RP offers much better distributed performance than RC, and achieves a peak of 270–274 up/s for GC-M, depending on the routing.

We see a drop in the absolute throughput values for GI-S and GC-W compared to GC-M at 222 up/s and 227 up/s for RP. We also notice a sharp increase in the batch latency of RC for GC-W, from ≈ 75 seconds for GC-M and GI-S to ≈ 110 seconds for GC-W. RP undergoes a similar, although modest, rise from 3.6 seconds for GC-M to 4.4 seconds for both GI-S and GC-W. This is because of the nature of the workloads. While GI-S needs to aggregate the embeddings of the vertices to the embeddings of the in-neighbors, GC-W needs to perform weighted aggregation of all the in-neighbors. The observed throughput speedup of RP over RC is a result of significant reductions in both computation and communication times per batch, e.g., a $20.5\times$ and $20\times$ drop in computation and communication times for GC-M using the streaming partitioner (Fig. 16, right subfigure).

We observe that the throughput for the distributed execution is much smaller than a single-machine setup, e.g., dropping from 10.3K up/s for a single-machine setup to 7K up/s on 4 workers for a 3-layer GC-M on the Arxiv graph. This is due to network, rather than in-memory, message passing, and also the need for barrier-synchronized execution required to send halo messages and perform compute at each hop.

6.3.2 Impact of Number of Partitions

Fig. 18 evaluates strong scaling of the systems with an increase in partitions from 4 to 16 for RP and RC, on GC-M with $bs = 1000$. As the number of partitions increases, the throughput (bar, left y-axis, log scale) shows *strong scaling* for both RC and RP. RC scales from 7.3 up/s to 23.2 up/s from 4–16 partitions, with a $3.2\times$ scaling and an 80% scaling efficiency. RP goes from 130 up/s to 400 up/s for 4–16 partitions, which is a $3.1\times$ speedup at 77% efficiency, which holds for both routing strategies. The scaling efficiency is ideal from 4 to 6 workers, at 102% for RC and 109% for RP, and competitive at 8 workers (92% and 104%), after which it gradually reduces. That said, the magnitude of throughput for RP is $17\times$ higher than RC.

Achieving strong scaling is not always possible in distributed systems since communication costs often increase super-linearly with the number of machines, mitigating benefits. However, in our case, as partitions increase, the batch is split into smaller batches across workers, with each taking lesser compute time to process. The compute times (green marker, right y-axis, log scale) drop from 75 seconds to ≈ 19 seconds for RC, and from 4 seconds to 1.4 seconds for RP

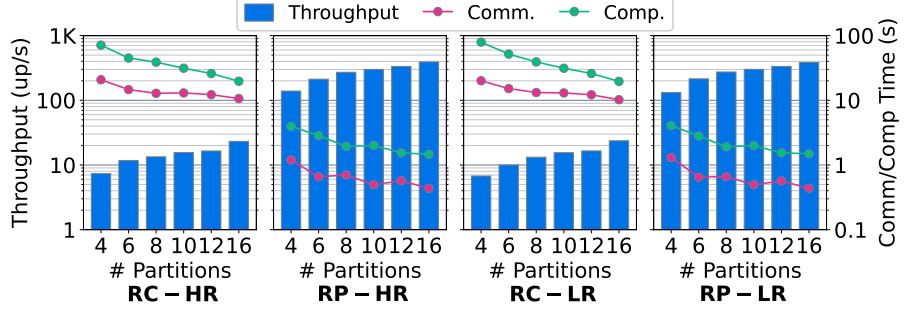


Figure 18: Distributed performance of RP and RC on 3-layer GC-M for Papers, $bs = 1000$ and 4–16 partitions.

as partitions grow from 4–16. At the same time, the communication time also reduces since the number of vertices that must be exchanged between workers decreases with smaller batches per worker. These drop by $\approx 2\times$ for RC from 20 seconds to ≈ 10 seconds (*pink marker, right y-axis, log scale*) and by $\approx 2.9\times$ for RP from 1.25 seconds to 0.44 seconds. RP benefits more from a drop in communications time since RC has a higher communication overhead as it pulls all remote in-neighbors at each hop. As a result, communications forms 40% of its total latency compared to 29% for RP.

6.3.3 Impact of Routing Strategies

Fig. 17 compares the performance of the hash-based (HR) and locality-aware routing (LR) strategies at the server, for the GC-M workload on Papers graph with $bs = 1000$ and 8 partitions. The high-degree set is updated after every 500K updates. Both strategies start with the same METIS-partitioned 80% of the original graph, and the same number of edge cuts. We report the relative reduction in edge cuts for LR compared to HR (*red line, left y-axis*) after every additional 10% of the 5M update events are received. LR monotonically shows a steady improvement in edge cuts over HR, with about 50K fewer edge cuts after 50% of updates, and 106K fewer cuts after all updates are received. In the real world, where graph sizes will continue to increase as the stream arrives, this will lead to a steadily increasing partitioning benefit for LR.

The reduction in edge cuts also leads to a better throughput for LR over HR, though it is marginal at 1.5% on average (*yellow and green lines, right y-axis*), e.g., after 60% updates, LR has a throughput of 281 up/s while HR has 275 up/s. While the lower edge cuts translate to fewer communications for LR compared to HR, it does not translate to higher throughput. This is because the batch latencies for both RC and RP are dominated by a *straggler worker* 5 (Fig. 16, right subfigure), whose execution time is compute-bound rather than communication-bound. Since we use a synchronized BSP execution, this client slows down the end-to-end execution, and mitigates edge-cut benefits for this graph.

7 Related Work

GNNs have found numerous applications due to their ability to learn low-level representations of graph data. E-commerce platforms like Alibaba leverage GNNs to analyze user behavior and deliver personalized product recommendations [55]. Social media platforms like Pinterest utilize GNNs for content recommendation to users [48]. Google applies GNNs in estimating travel times for Google Maps [13]. In this work, we focus on GNN applications over large dynamic graphs with millions–billions of vertices and edges, receiving streaming updates on the order of 100–1000s of updates per second, as seen commonly in social, e-commerce, fintech, and road networks.

Research on GNN inference and serving has largely been limited to *static graphs* [47, 53],

where the graph structure and vertex/edge features do not change over time. Popular frameworks like DGL [41] and Pytorch Geometric [15] are primarily designed for GNN training and are not optimized for GNN serving. DGI [47] proposes a *layer-wise* inference approach, which computes embeddings layer-by-layer and handles the tasks of all target vertices in the same layer batch-by-batch. This avoids the neighborhood explosion problem encountered while adopting *vertex-wise* inference. Frameworks such as GNNIE [33] and GraphAGILE [50] introduce specialized hardware accelerators designed to enable low-latency GNN inference, while ViTeGNN [54] introduces an algorithm-model-architecture co-design to support low-latency GNN inference on graphs with temporal properties on FPGAs. Hu et al. [26] propose λ -Grapher, which is a serverless system for GNN serving that achieves resource efficiency through computation graph sharing and fine-grained resource allocation for the separate memory and compute-bound requirements of a GNN layer. These methods, however, are non-trivial to extend to evolving graphs.

Real-world graphs are often dynamic in nature and require specialized frameworks. *Streaming and temporal graph analytics* has been extensively studied in literature for traditional algorithms like PageRank and ShortestPath [4, 19, 32, 39], and even incremental graph processing frameworks exist [5]. Applications like PageRank on streaming graphs negate the influence of a vertex’s previous state before propagating its updated state in each iteration. However, traditional solutions for streaming graph analytics are not directly applicable to GNN inference [42] since GNNs handle large hidden states, making computation and memory footprint more demanding. Also, graph updates can extend to L -hops per update rather than being limited to immediate neighbors. This necessitates specialized approaches to streaming graph GNN inference.

There is preliminary work on GNN processing for *streaming graphs*. DGNN [29] proposes an LSTM-inspired architecture to capture the dynamic nature of evolving graphs, but is limited to GNN training. OMEGA [22] proposes selective recomputation of embeddings using a heuristic to minimize the approximation errors due to stale precomputed embeddings. They also offer parallelism strategies for graph calculations to balance inference latency and accuracy. Helios [37] solves *request-based* low-latency online inference for GNNs by pre-sampling during graph updates and maintaining a query-aware sample cache to reduce the sampling overhead at inference time. STAG [40] also solves the *request-based* inference problem using a collaborative serving mechanism that balances the inference and staleness latencies. In contrast, RIPPLE++ does *trigger-based* inference while performing *exact* (not approximate), *full neighborhood* embeddings update.

A recent work, InkStream [42], is an incremental framework for GNN inference on dynamic graphs that also attempts to avoid redundant computation by “propagating only when necessary” and “fetching only the necessary”. Its event-based design enables pruning of update propagation, and for models with monotonic aggregation functions (e.g., *max*, *min*), it reduces the update scope by focusing on the affected region instead of the entire l -hop neighborhood. However, it suffers from several limitations. It lacks support for attention-based architectures and restricts updates to only edge additions and deletions. Also, it assumes that all updates are available *a priori* and processes them as a single batch, which is unrealistic in a streaming setting. It does not have a distributed execution model, limiting scalability when graphs do not fit on one machine. Our RIPPLE++ approach overcomes all these limitations, and, as we demonstrate, out-performs InkStream.

Further, none of these methods evaluate their solutions on large graphs with millions of vertices and 100M+ edges. So their scalability on single machines or in a distributed setting remains unknown. The largest public graph for GNNs, Papers [18], is itself modest in size compared to web-scale graphs that can exceed the RAM of a single machine when considering their features and embeddings. This highlights the scalability challenges for GNN inference over large graphs.

8 Conclusions

In this work, we present a novel framework, RIPPLE++, to efficiently perform GNN inference over large-scale streaming graphs. Unlike traditional methods that rely on exhaustive look-back computations, our approach adopts a strictly look-forward incremental computation, where vertices are first-class entities that manage their data and updates. RIPPLE++ is able to process $\approx 56K$ up/s for sparser graphs like Arxiv and up to $7.6K$ up/s for larger and denser graphs like Products on a single machine. Its distributed variant supports larger graphs and exhibits strong scaling, albeit at a lower throughput. As future work, we plan to explore other streaming partitioning and routing strategies to maintain balanced partitions as the graph changes, and support dynamic batch sizes for latency-sensitive tasks. Lastly, we also intend to explore how RIPPLE++’s incremental strategy could be extended to an approximate inference setup where all neighbor aggregation is avoided, in return for improved performance.

Acknowledgments

The authors thank Roopkatha Banerjee, Tejas C., Prashanthi S.K., and other members of the DREAM:Lab, Indian Institute of Science, for their assistance and insightful feedback.

References

- [1] Khaled Ammar. Techniques and systems for large dynamic graphs. In *2016 on SIGMOD’16 Ph.D. Symposium*, 2016.
- [2] Khaled Ammar. Techniques and systems for large dynamic graphs. In *2016 on SIGMOD’16 Ph.D. Symposium*, 2016.
- [3] Ting Bai, Youjie Zhang, Bin Wu, and Jian-Yun Nie. Temporal graph neural networks for social recommendation. In *2020 IEEE International Conference on Big Data (Big Data)*, 2020.
- [4] Maciej Besta, Marc Fischer, Vasiliki Kalavri, Michael Kapralov, and Torsten Hoefer. Practice of streaming processing of dynamic graphs: Concepts, models, and systems. *IEEE Trans. Parallel Distrib. Syst. (TPDS)*, 2023.
- [5] Ruchi Bhoot, Suved Sanjay Ghammode, and Yogesh Simmhan. Taris: Scalable incremental processing of time-respecting algorithms on streaming graphs. *IEEE Trans. on Parallel and Distr. Sys. (TPDS)*, 2024.
- [6] Ruchi Bhoot, Tuhin Khare, Manoj Agarwal, Siddharth Jaiswal, and Yogesh Simmhan. Triparts: Scalable streaming graph partitioning to enhance community structure. *VLDB Endowment*, 2025.
- [7] Zhenkun Cai, Xiao Yan, Yidi Wu, Kaihao Ma, James Cheng, and Fan Yu. Dgcl: an efficient communication library for distributed gnn training. In *Sixteenth European Conference on Computer Systems*, 2021.
- [8] Jianxin Chang, Chen Gao, Yu Zheng, Yiqun Hui, Yanan Niu, Yang Song, Depeng Jin, and Yong Li. Sequential recommendation with graph neural networks. In *ACM SIGIR Conf. on Research and Development in Info. Retrieval*, 2021.
- [9] Bo Chen, Wei Guo, Ruiming Tang, Xin Xin, Yue Ding, Xiuqiang He, and Dong Wang. Tgcn: Tag graph convolutional network for tag-aware recommendation. In *ACM Intl. Conf. on Information & Know. Management (CIKM)*, 2020.
- [10] Avery Ching, Sergey Edunov, Maja Kabiljo, Dionysios Logothetis, and Sambavi Muthukrishnan. One trillion edges: Graph processing at facebook-scale. *VLDB Endowment*, 2015.
- [11] Gabriele Corso, Luca Cavalleri, Dominique Beaini, Pietro Liò, and Petar Velickovic. Principal neighbourhood aggregation for graph nets. In *Intl. Conf. on Neural Info. Proc. Sys. (NeurIPS)*, 2020.
- [12] Nima Dehmamy, Albert-László Barabási, and Rose Yu. Understanding the representation power of graph neural networks in learning graph topology. In *Intl. Conf. on Neural Info. Proc. Sys. (NeurIPS)*, 2019.
- [13] Austin Derrow-Pinion, Jennifer She, David Wong, Oliver Lange, Todd Hester, Luis Perez, Marc Nunkesser, Seongjae Lee, Xueying Guo, Brett Wiltshire, Peter W. Battaglia, Vishal Gupta, Ang Li, Zhongwen Xu, Alvaro Sanchez-Gonzalez, Yujia Li, and Petar Velivcković. Eta prediction with graph neural networks in google maps. In *ACM Intl. Conf. on Information & Know. Management (CIKM)*, 2021.
- [14] Yingtong Dou, Zhiwei Liu, Li Sun, Yutong Deng, Hao Peng, and Philip S. Yu. Enhancing graph neural network-based fraud detectors against camouflaged fraudsters. In *ACM Intl. Conf. on Info. & Know. Management (CIKM)*, 2020.

- [15] Matthias Fey and Jan Eric Lenssen. Fast graph representation learning with pytorch geometric. *arXiv preprint arXiv:1903.02428*, 2019.
- [16] Shengnan Guo, Youfang Lin, Ning Feng, Chao Song, and Huaiyu Wan. Attention based spatial-temporal graph convolutional networks for traffic flow forecasting. In *AAAI Conference on Artificial Intelligence*, 2019.
- [17] William L. Hamilton, Rex Ying, and Jure Leskovec. Inductive representation learning on large graphs. In *Intl. Conf. on Neural Info. Proc. Sys. (NeurIPS)*, 2017.
- [18] Weihua Hu, Matthias Fey, Marinka Zitnik, Yuxiao Dong, Hongyu Ren, Bowen Liu, Michele Catasta, and Jure Leskovec. Open graph benchmark: datasets for machine learning on graphs. In *Intl. Conf. on Neural Info. Proc. Sys. (NeurIPS)*, 2020.
- [19] Chengying Huan, Yongchao Liu, Heng Zhang, Hang Liu, Shiyang Chen, Shuaiwen Leon Song, and Yanjun Wu. Tegraph+: Scalable temporal graph processing enabling flexible edge modifications. *IEEE Trans. on Parallel and Distr. Sys. (TPDS)*, 2024.
- [20] Tim Kaler, Nickolas Stathas, Anne Ouyang, Alexandros-Stavros Iliopoulos, Tao Schardl, Charles E Leiserson, and Jie Chen. Accelerating training and inference of graph neural networks with fast sampling and pipelining. *Proceedings of Machine Learning and Systems (PMLR)*, 2022.
- [21] George Karypis and Vipin Kumar. Metis - a software package for partitioning unstructured graphs, partitioning meshes and computing fill-reducing ordering of sparse matrices. Technical Report 97-061, University of Minnesota, 1997.
- [22] Geon-Woo Kim, Donghyun Kim, Jeongyo Moon, Henry Liu, Tarannum Khan, Anand Iyer, Daehyeok Kim, and Aditya Akella. Omega: A low-latency gnn serving system for large graphs. *arXiv preprint arXiv:2501.08547*, 2025.
- [23] Thomas N. Kipf and Max Welling. Semi-supervised classification with graph convolutional networks. In *Intl. Conf. on Learning Rep. (ICLR)*, 2017.
- [24] Dandan Lin, Shijie Sun, Jingtao Ding, Xuehan Ke, Hao Gu, Xing Huang, Chonggang Song, Xuri Zhang, Lingling Yi, Jie Wen, and Chuan Chen. Platogl: Effective and scalable deep graph learning system for graph-enhanced real-time recommendation. In *ACM Intl. Conf. on Information & Know. Management (CIKM)*, 2022.
- [25] Yang Liu, Xiang Ao, Zidi Qin, Jianfeng Chi, Jinghua Feng, Hao Yang, and Qing He. Pick and choose: A gnn-based imbalanced learning approach for fraud detection. In *Web Conference 2021*, 2021.
- [26] Mingxuan Lu, Zhichao Han, Susie Xi Rao, Zitao Zhang, Yang Zhao, Yinan Shan, Ramesh Raghunathan, Ce Zhang, and Jiawei Jiang. Bright - graph neural networks in real-time fraud detection. In *ACM Intl. Conf. on Information & Know. Management (CIKM)*, 2022.
- [27] Xinze Lyu, Guangyao Li, Jiacheng Huang, and Wei Hu. Rule-guided graph neural networks for recommender systems. In *Intl. Semantic Web Conf (ICWS)*, 2020.
- [28] Lingxiao Ma, Zhi Yang, Youshan Miao, Jilong Xue, Ming Wu, Lidong Zhou, and Yafei Dai. Neugraph: parallel deep neural network computation on large graphs. In *USENIX Annual Technical Conference (ATC)*, 2019.
- [29] Yao Ma, Ziyi Guo, Zhaocun Ren, Jiliang Tang, and Dawei Yin. Streaming graph neural networks. In *ACM SIGIR Conf. on Research and Development in Info. Retrieval*. Association for Computing Machinery, 2020.

[30] Ananth Mahadevan and Michael Mathioudakis. Cost-aware retraining for machine learning. *Knowledge-Based Systems*, 2024.

[31] Grzegorz Malewicz, Matthew H Austern, Aart JC Bik, James C Dehnert, Ilan Horn, Naty Leiser, and Grzegorz Czajkowski. Pregel: a system for large-scale graph processing. In *ACM SIGMOD Intl. Conf. on Management of data*, 2010.

[32] Mugilan Mariappan, Joanna Che, and Keval Vora. Dzig: sparsity-aware incremental processing of streaming graphs. In *ACM European Conference on Computer Systems (EuroSys)*, 2021.

[33] Sudipta Mondal, Susmita Dey Manasi, Kishor Kunal, Ramprasath S, and Sachin S. Sapatinakar. Gnnie: Gnn inference engine with load-balancing and graph-specific caching. In *ACM/IEEE Design Automation Conference (DAC)*, 2022.

[34] Pranjal Naman and Yogesh Simmhan. Ripple: Scalable Incremental GNN Inferencing on Large Streaming Graphs . In *IEEE 45th International Conference on Distributed Computing Systems (ICDCS)*, 2025.

[35] Morteza Ramezani, Weilin Cong, Mehrdad Mahdavi, Mahmut T. Kandemir, and Anand Sivasubramaniam. Learn locally, correct globally: A distributed algorithm for training graph neural networks. In *Intl. Conf. on Learning Rep. (ICLR)*, 2022.

[36] Zixing Song, Yuji Zhang, and Irwin King. Towards fair financial services for all: A temporal gnn approach for individual fairness on transaction networks. In *ACM Intl. Conf. on Information & Know. Management (CIKM)*, 2023.

[37] Jie Sun, Zuocheng Shi, Li Su, Wenting Shen, Zeke Wang, Yong Li, Wenyuan Yu, Wei Lin, Fei Wu, Bingsheng He, and Jingren Zhou. Helios: Efficient distributed dynamic graph sampling for online gnn inference. In *ACM SIGPLAN Annual Symp. on Prin. and Practice of Parallel Prog. (PPoPP)*, 2025.

[38] Petar Veličković, Guillem Cucurull, Arantxa Casanova, Adriana Romero, Pietro Liò, and Yoshua Bengio. Graph attention networks. In *Intl. Conf. on Learning Rep. (ICLR)*, 2018.

[39] Keval Vora, Rajiv Gupta, and Guoqing Xu. Kickstarter: Fast and accurate computations on streaming graphs via trimmed approximations. In *SIGARCH Comput. Archit. News*, 2017.

[40] Jiawen Wang, Quan Chen, Deze Zeng, Zhuo Song, Chen Chen, and Minyi Guo. Stag: Enabling low latency and low staleness of gnn-based services with dynamic graphs. In *IEEE International Conference on Computer Design (ICCD)*, 2023.

[41] Minjie Wang, Da Zheng, Zihao Ye, Quan Gan, Mufei Li, Xiang Song, Jinjing Zhou, Chao Ma, Lingfan Yu, Yu Gai, et al. Deep graph library: A graph-centric, highly-performant package for graph neural networks. *arXiv preprint arXiv:1909.01315*, 2019.

[42] Dan Wu, Zhaoying Li, and Tulika Mitra. Inkstream: Instantaneous gnn inference on dynamic graphs via incremental update. In *2025 IEEE International Parallel and Distributed Processing Symposium (IPDPS)*, 2025.

[43] Shiwen Wu, Fei Sun, Wentao Zhang, Xu Xie, and Bin Cui. Graph neural networks in recommender systems: A survey. *ACM Comput. Surv.*, 2022.

[44] Yinjun Wu, Edgar Dobriban, and Susan Davidson. DeltaGrad: Rapid retraining of machine learning models. In *Intl. Conf. on Machine Learning (ICML)*, 2020.

[45] Keyulu Xu, Weihua Hu, Jure Leskovec, and Stefanie Jegelka. How powerful are graph neural networks? In *Intl. Conf. on Learning Rep. (ICLR)*, 2019.

[46] Liangwei Yang, Zhiwei Liu, Yingtong Dou, Jing Ma, and Philip S. Yu. Consisrec: Enhancing gnn for social recommendation via consistent neighbor aggregation. In *ACM SIGIR Conf. on Research and Development in Info. Retrieval*, 2021.

[47] Peiqi Yin, Xiao Yan, Jinjing Zhou, Qiang Fu, Zhenkun Cai, James Cheng, Bo Tang, and Minjie Wang. Dgi: An easy and efficient framework for gnn model evaluation. In *ACM SIGKDD Conf. on Know. Disc. and Data Mining (KDD)*, 2023.

[48] Rex Ying, Ruining He, Kaifeng Chen, Pong Eksombatchai, William L. Hamilton, and Jure Leskovec. Graph convolutional neural networks for web-scale recommender systems. In *ACM SIGKDD Conf. on Know. Disc. and Data Mining (KDD)*, 2018.

[49] Hao Yuan, Yajiong Liu, Yanfeng Zhang, Xin Ai, Qiange Wang, Chaoyi Chen, Yu Gu, and Ge Yu. Comprehensive evaluation of gnn training systems: A data management perspective. *Proc. VLDB Endow.*, 2024.

[50] Bingyi Zhang, Hanqing Zeng, and Viktor K. Prasanna. GraphAGILE: An FPGA-Based Overlay Accelerator for Low-Latency GNN Inference . *IEEE Trans. on Parallel and Distr. Sys. (TPDS)*, 2023.

[51] Lizhi Zhang, Zhiquan Lai, Shengwei Li, Yu Tang, Feng Liu, and Dongsheng Li. 2pgraph: Accelerating gnn training over large graphs on gpu clusters. In *2021 IEEE International Conference on Cluster Computing (CLUSTER)*, 2021.

[52] Da Zheng, Chao Ma, Minjie Wang, Jinjing Zhou, Qidong Su, Xiang Song, Quan Gan, Zheng Zhang, and George Karypis. DistDGL: Distributed Graph Neural Network Training for Billion-Scale Graphs. In *IEEE/ACM 10th Workshop on Irregular Applications: Architectures and Algorithms (IA3)*, 2020.

[53] Hongkuan Zhou, Ajitesh Srivastava, Hanqing Zeng, Rajgopal Kannan, and Viktor Prasanna. Accelerating large scale real-time gnn inference using channel pruning. *Proc. VLDB Endow.*, 2021.

[54] Hongkuan Zhou, Bingyi Zhang, Rajgopal Kannan, Carl Busart, and Viktor K. Prasanna. Vitegnn: Towards versatile inference of temporal graph neural networks on fpga. *IEEE Trans. on Parallel and Distr. Sys. (TPDS)*, 2025.

[55] Rong Zhu, Kun Zhao, Hongxia Yang, Wei Lin, Chang Zhou, Baole Ai, Yong Li, and Jingren Zhou. Aligraph: a comprehensive graph neural network platform. *Proc. VLDB Endow.*, 2019.

9 Appendix

Here, we provide additional results and discussions supporting the main text. In particular, we present detailed experiments demonstrating that our **RC** and **DRC** implementations serve as strong and fair baselines for **RIPPLE++**, along with comparisons with other DGL-based baselines on both CPU and GPU.

9.1 Comparison with Vertex- and Layer-wise Inference

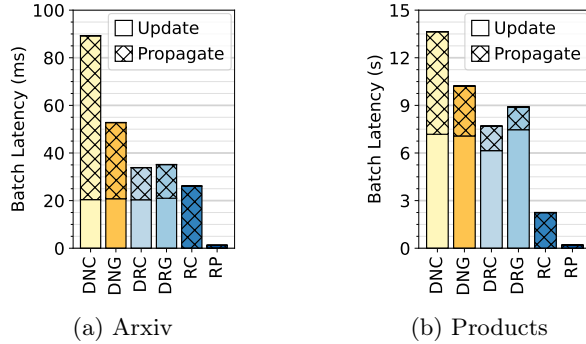


Figure 19: Comparison of DGL’s vertex- and layer-wise recompute, our layer-wise recompute (RC), and **RIPPLE++**’s (RP) incremental compute on CPU and CPU+GPU for 3-layer GC-S and $bs = 10$ on Arxiv and Products graphs.

We first compare DGL’s vertex-wise inference on the CPU (**DNC**) and CPU+GPU (**DNG**), with its layer-wise recompute strategy on the CPU (**DRC**) and CPU+GPU (**DRG**). For the CPU+GPU configurations, the computation graphs are built on the CPU while the forward pass of inference takes place on the GPU, as is standard practice [41, 49, 52]. Further, we also contrast these against our implementation of layer-wise recompute (**RC**) and the **RIPPLE++** incremental strategies (**RP**) run on the CPU. All of these execute on the GPU workstation using a single-machine execution model.

Fig. 19 shows the median batch latency of processing 100 batches of 10 updates each by these strategies for the Arxiv and Products graphs. The vertex-wise inference strategies DNC and DNG, compared against their corresponding layer-wise recompute strategies DRC and DRG are significantly slower, by $\approx 2.6\times$ and $\approx 1.8\times$ on the CPU, $\approx 1.5\times$ and $\approx 1.12\times$ on the CPU+GPU, for Arxiv and Products, respectively. This is because of the redundant computations that are performed for each batch in vertex-wise inference. Also, the GPU-based DRG method offers limited benefits over the CPU-based DRC strategy. Since the layer-wise strategy processes embeddings one layer at a time, it only requires data for the immediate previous layer in the computation graph. Due to these small batch sizes, the computational workload is minimal, which limits the performance gains from GPU-based computation, leading to similar performance for Arxiv, and $\approx 1.1\times$ slower for Products. This justifies our choice of a layer-wise approach and just using CPUs.

Further, our own custom layer-wise recompute implementation on CPU (**RC**) is $\approx 1.4\text{--}4\times$ faster than both the CPU and GPU versions of DGL’s layer-wise recompute (**DRC**, **DRG**). While DGL’s graph APIs ease the development of GNN training models, they are not optimized for handling a stream of updates. DGL uses sparse matrix formats for its internal graph representation. It accepts graph structures as COO matrices but internally compiles them into more efficient CSR/CSC formats for computation. Since DGL’s internal structures are largely immutable, graph updates cause the entire graph structure to be rebuilt for every update ⁵.

⁵<https://github.com/dmlc/dgl/blob/master/python/dgl/heterograph.py>

Moreover, multiple types of updates in a batch can lead to multiple graph updates within a batch. As a result, updating the graph topology consumes a significant amount of time (*Update* stack in Fig. 19). In contrast, our RC implementation uses lightweight edge-list structures designed to efficiently handle streaming updates. They offer much faster update times and comparable or slightly slower than the compute propagation times. The incremental computation of RIPPLE++ (RP) is substantially faster than all of these. In the rest of the experiments, we use DRC and RC running on the CPU as the competitive baselines to compare against RIPPLE++’s incremental approach.